Clays and Clay Minerals, Vol. 46, No. 4, 379–399, 1998.

COMPARATIVE STUDY OF THE MOBILITY OF MAJOR AND TRACE ELEMENTS DURING ALTERATION OF AN ANDESITE AND A RHYOLITE TO BENTONITE, IN THE ISLANDS OF MILOS AND KIMOLOS, AEGEAN, GREECE

GEORGE E. CHRISTIDIS

Technical University of Crete, Department of Mineral Resources Engineering, Kounoupidiana, 73100 Chania, Crete, Greece

Abstract—Progressive alteration by seawater of an andesite in the Aegean Island of Milos and an ignimbrite in the Aegean Island of Kimolos, Greece, formed bentonites with or without zeolites. Both profiles are dominated by migration of alkalis and uptake of Mg, Fe and H_2O, while Al and Ti are immobile. The relative removal of alkalis controls the formation of either smectite or zeolites. The behavior of Ca and Si depends on the chemistry of the parent rock. In the rhyolitic profile, alteration is controlled by gain of Mg, Fe^{2+} and Ca and loss of Na, K and Si, while in the andesitic profile by gain of Mg and Fe^{2+} and loss of Na, K and Ca. In both profiles, significant uptake of $SO_4^{=}$ was not observed. Moreover Zr, Nb, V and Ni are immobile and have been enriched residually, while Sr, Rb and Y are lost in both profiles. Thorium is immobile in the rhyolitic profile but is leached in the andesitic profile. Also, the rare earth elements (REE) display fractionation in both profiles; the degree of fractionation increases with the degree of alteration to bentonite. Fractionation of the REE in both profiles and mobility of Th in the andesitic profile are related to the existence of monazite (rhyolitic profile) and apatite (andesite profile). The REE and Th appear to partition into phosphates rather than smectite.

The mobility of Y coupled with the immobility of Nb increases the Nb : Y ratio with advancing alteration, rendering discrimination diagrams that use this ratio to determine the nature of the protoliths misleading. Mass balance calculations showed that in the smectite-rich zones the water : rock (WR) ratio might be as high as 13:1 in both profiles, while in the zeolite-bearing zones it is about 5.5:1. Such WR ratios explain the observed extensive mass transfer and suggest that the pore fluid chemistry might overprint the chemical characteristics of the parent rocks controlling smectite and bentonite chemistry.

Key Words—Alteration, Andesite, Bentonite, Element Mobilization, Mordenite, Phosphates, REE Fractionation, Residual Enrichment, Rhyolite, Smectite, Water : Rock Ratio.

INTRODUCTION

The alteration of volcanic glass yields smectites and various types of zeolites (Sheppard and Gude 1968, 1973; Boles and Surdam 1979; Iijima 1980; Senkayi et al. 1984; Hay and Guldman 1987; Noh and Boles 1989; Altaner and Grim 1990; Christidis et al. 1995), leading to the formation of economic deposits of either bentonites or zeolites (Mumpton 1977; Grim and Güven 1978). Alteration of volcanic glass may take place through weathering, gas phase crystallization, burial diagenesis, contact metamorphism, hydrothermal activity, percolating groundwater and, in alkaline lakes or the sea floor, in marine sediments (Iijima 1980; Cas and Wright 1988).

Field observations (Zielinski 1982; Senkayi et al. 1984; Christidis et al. 1995) and laboratory experiments (Mottl and Holland 1978; Seyfried and Mottl 1982; Shiraki et al. 1987; Shiraki and Iijama 1990) have shown that the conversion of volcanic glass to either smectites or zeolites involves mobilization of elements from and to the altered glass. Thus the loss of alkalis and a high Mg-activity promote the formation of smectite (Hay 1977; Senkayi et al. 1984). When leaching is not effective, zeolites crystallize usually from precursor gels (Mariner and Surdam 1970; Surdam 1977; Taylor and Surdam 1981; Steefel and van Cappellen 1990), while smectite generally forms in the initial stages of the alteration (Sheppard and Gude 1968, 1973; Dibble and Tiller 1981; Hay and Guldman 1987). Leaching of Si from acidic rocks might lead to bentonites without silica polymorphs (Zielinski 1982; Christidis and Scott 1997). When excess Si remains in the system, opal-CT forms (Henderson et al. 1971; Christidis and Dunham, 1997).

The chemistry of the parent rock controls both the type and the composition of reaction products (Iijima 1980; Christidis and Dunham 1993, 1997). Intermediate rocks tend to form Wyoming- and Chambers-type montmorillonite, whereas their acidic counterparts tend to form beidellite and Tatatilla-type montmorillonite (Christidis and Dunham 1993, 1997). However, this does not seem to be always the case. Recently Christidis and Scott (1997) described the formation of Chambers-type montmorillonite by alteration of an ignimbrite. This indicates that, in open systems, the introduction of key chemical elements might influence the composition of the neoformed smectites and, consequently, the alteration of the parent rock.

Although the mineralogical and major chemical features of the formation of bentonites have been studied

Copyright © 1998, The Clay Minerals Society

https://doi.org/10.1346/CCMN.1998.0460403 Published online by Cambridge University Press

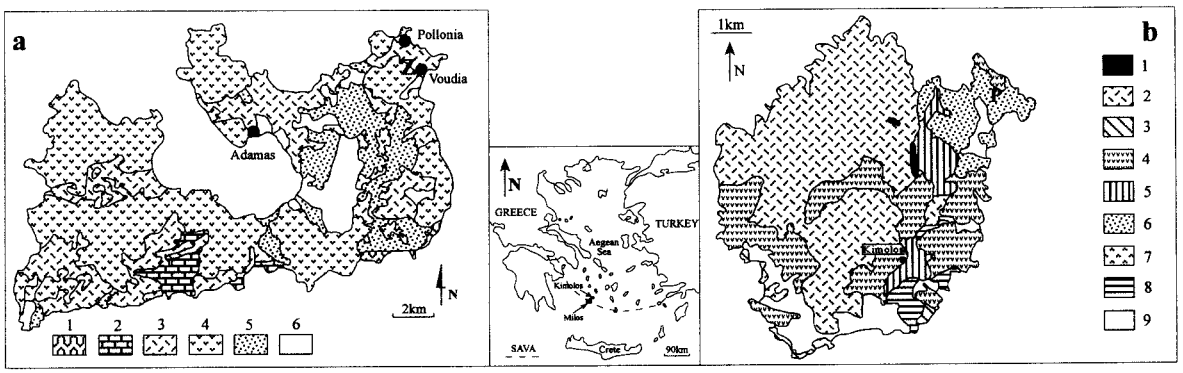

Figure 1. Simplified geological map of the sampling areas. a) Milos, modified after Fyticas et al. (1986). Key to the numbers: 1 = Metamorphic basement, 2 = Neogene sedimentary sequence, 3 = Upper Pleiocene-Lower Pleistocene pyroclastic rocks (undifferentiated), 4 = Upper Pleiocene-Lower Pleistocene lavas (undifferentiated), 5 = Upper Pleistocene chaotic horizon, 6 = Alluvial deposits, Z = Zoulias deposit. b) Kimolos modified after Fyticas and Vougioukalakis (1993). Key to the numbers: 1 = Granite, 2 = Kastro ignimbrite, 3 = Hydrothermally altered volcanic rocks, 4 = Lavas undifferentiated, 5 = Pyroclastic breccia, 6 = Ignimbrite of Prassa area, 7 = Pumice flows, 8 = Pyroclastics of Psathi area, 9 = Alluvial scree, and elluvial deposits, P = Prassa deposit.

thoroughly, the mobility of trace elements including lanthanides, with few exceptions (Zielinski 1982; Elliott 1993), have been examined thoroughly only in weathering profiles (Duddy 1980; Banfield and Eggleton 1989; Prudencio et al. 1995). This contribution examines 2 alteration profiles in the volcanic islands of Milos and Kimolos, Aegean, Greece, in which an andesite and a rhyolitic ignimbrite have been converted to bentonite in a submarine environment. Its purpose is to 1) describe mobilization of both major and trace elements including REE; 2) compare the geochemical behavior of chemical elements along both profiles; 3) examine and compare the interdependence of mineralogy and relative mobility of the various chemical elements in the 2 profiles; and 4) estimate the water: rock ratios and determine their significance during alteration.

GEOLOGICAL SETTING AND LOCATION OF THE STUDY AREAS

The islands Milos and Kimolos are situated in the SW part of the South Aegean Volcanic Arc (Figures 1a and 1b), which was created by the subduction of the African Plate under the deformed margin of the Eurasian Plate (Fyticas et al. 1986). The islands have similar geological history (Fyticas 1977; Fyticas et al. 1986; Fyticas and Vougioukalakis 1993).

On Milos Island, the study area is located in the composite Zoulias bentonite deposit (Figure 1a), which consists of 11 distinct horizons (Christidis et al. 1995). The alteration profile comprises the progressive alteration of an andesitic lava (Figure 2), which constitutes the lowest horizon of the deposit (Christidis et al. 1995). On Kimolos Island, the alteration profile was formed at the expense of the unwelded Prassa ignimbrite (Figure 1b), the alteration being structurally controlled. The profile can be subdivided into 6 different zones (Figure 2), which represent the gradual transition from the fresh glass to a gray bentonite and a white, zeolite-bearing bentonite. In both profiles, alteration took place in a submarine environment, at a low temperature (Christidis et al. 1995).

MATERIALS AND METHODS

In both profiles, samples were collected 30–40 cm beneath the surface to minimize weathering and contamination. Whole-rock mineralogy was determined by X-ray diffraction (XRD) using a Philips powder diffractometer equipped with a 1710 computerized control unit, operating at 40 kV and 30 mA, using Ni-filtered Cu$K\alpha$ radiation. Scanning speed was 1 °2θ/min. The clay mineralogy was determined after dispersion of the <2-μm fraction in distilled water using sodium polymetaphosphate. The clay fraction was separated, spread on glass slides and allowed to dry in atmospheric conditions. The slides were then saturated with ethylene glycol at 60 °C for at least 16 h to ensure maximum saturation.

Both the major and trace chemical elements were determined with wavelength dispersive (WD) X-ray fluorescence (XRF) spectroscopy. The major elements (Si, Ti, Al, Fe, Mn, Mg, Ca, Na, K and P) were analyzed using the method of Bennett and Oliver (1976) modified by N. Marsh, University of Leicester, using an ARL8420$^+$ WD/XRF spectrometer. The samples were fused using a flux: sample powder ratio of 1:5 and were casted in Al-dies forming glass beads. A mixture of 80% Li-tetraborate and 20% Li-metaborate was used as flux. The SO_3 was determined by means of a calibration curve made of standards prepared by addition of variable amounts of $BaSO_4$ in the form of

https://doi.org/10.1346/CCMN.1998.0460403 Published online by Cambridge University Press

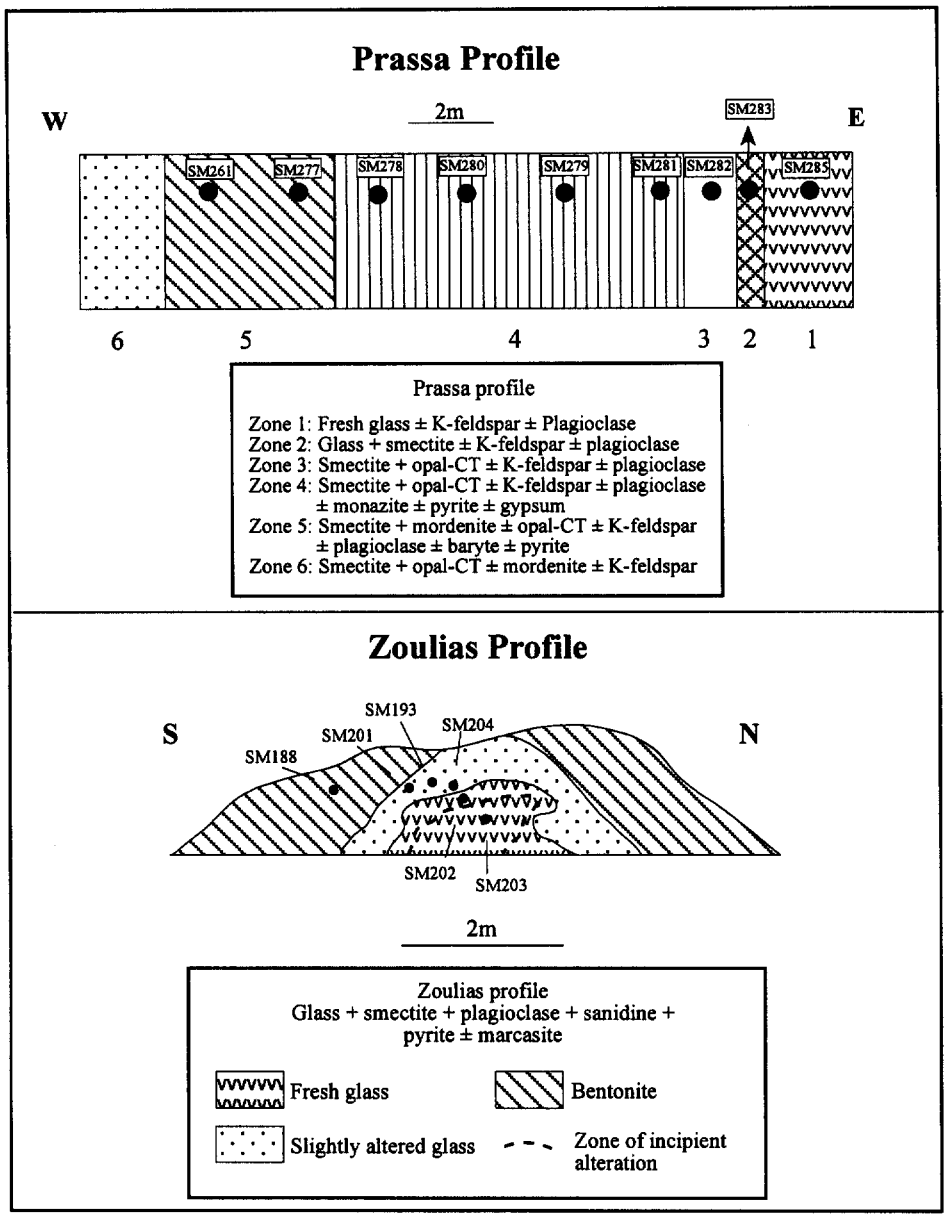

Figure 2. Schematic cross sections of the sampling sites and mineralogical composition of the alteration profiles studied.

barites, to a barite-free bentonite containing 153.5 ppm Ba.

Niobium, Zr, Y, Sr, Rb, Th, Zn, Ni, V, Cr and Ba were determined on pressed powder pellets using a Philips PW1400 XRF spectrometer. Rare earth element determination was carried out by inductively coupled plasma/optical emission (ICP/OE) spectrometry (Philips PV8060 simultaneous ICP/OE spectrometer), using the method of Walsh et al. (1981) modified at the University of Leicester. Analytical precision and accuracy for both major and trace elements were checked using a series of international standards. Typical values for the analytical methods and the instruments used are given by Pickering et al. (1993) and are listed in Table 1.

RESULTS

Mineralogy

The mineralogical composition of the profiles is summarized in Figure 2. The 6 different alteration zones observed in the Prassa profile correspond to different mineralogical assemblages. In both profiles, dioctahedral smectite has formed at the expense of vol-

https://doi.org/10.1346/CCMN.1998.0460403 Published online by Cambridge University Press

Table 1. Mean values and 1-sigma standard deviations for the major and trace elements determined on the ARL8420+ (major elements) and Philips PW1400 WD/XRF spectrometers, and the REE determined on the Philips V8060 ICP/OE spectrometer for various international standards; n = number of analyses, n.d. = not detectable (after Pickering et al. 1993).

	Major elements (%)											
	BOB-1 (n = 10)			NIM-G (n = 5)			JA-1 (n = 5)			SO-1 (n = 5)		
	Mean	Std dev	% Std dev	Mean	Std dev	% Std dev	Mean	Std dev	% Std dev	Mean	Std dev	% Std dev
SiO_2	50.59	0.1	0.2	77.75	0.49	0.63	66.06	0.27	0.41	59.09	0.53	0.9
TiO_2	1.29	0.05	0.35	0.1	0	0.2	0.88	0	0.57	0.91	0.01	0.66
Al_2O_3	16.40	0.04	0.24	11.52	0.07	0.63	14.35	0.05	0.32	18.13	0.1	0.56
Fe_2O_3	8.55	0.01	0.16	2.02	0.02	1.04	7.05	0.02	0.23	9.04	0.01	0.14
MnO	0.14	0	0.96	0.01	0	15.38	0.14	0	0.71	0.12	0	1.67
MgO	7.66	0.03	0.34	0.09	0.01	13.33	1.61	0.02	0.99	4.1	0.03	0.76
CaO	11.13	0.02	0.21	0.75	0	0.4	5.68	0.03	0.48	2.62	0.01	0.57
Na_2O	3.12	0.01	0.4	2.91	0.01	0.34	3.30	0.03	0.88	2.34	0.02	0.9
K_2O	0.37	0	0.32	4.94	0.01	0.24	0.75	0	0.40	3.28	0.02	0.64
P_2O_5	0.16	0	0.92	0.01	0	6.0	0.17	0	1.21	0.16	0	1.25
	Trace elements (ppm)											
	NIM-G (n = 8)			JA-1 (n = 5)			SO-1 (n = 10)			SO-2 (n = 8)		
	Mean	Std dev	% Std dev	Mean	Std dev	% Std dev	Mean	Std dev	% Std dev	Mean	Std dev	% Std dev
Nb	51.51	3.45	6.7	7.14	2.42	33.88	16.6	2.86	17.22	30.34	2.63	8.67
Zr	271.57	9.46	3.48	85.1	2.52	2.96	98.18	3.7	3.77	953.28	63.62	6.67
Y	152.4	5.56	3.65	32.2	2.82	8.8	26.55	3.86	14.54	54.09	4.75	8.79
Sr	11.32	1.27	11.25	249.68	1.92	0.77	330.92	9.85	2.98	356.99	19.35	5.42
Rb	324.69	8.6	2.65	6.3	1.25	19.9	142.97	7.12	4.98	78.59	8.49	10.81
Th	50.47	3.31	6.57	3.5	2.73	78.08	19.43	3.53	18.16	6.2	4.44	71.53
Ga	22.96	2.81	12.25	19.86	1.21	6.11	19.96	1.7	8.51	24.25	1.68	6.92
Zn	62.3	1.34	2.15	108.8	2.03	1.86	181.11	21.16	11.69	141.25	4.56	3.23
Ni	0.19	0.23	120.55	0.72	0.9	125.28	97.39	9.62	9.88	4.49	2.96	65.89
Sc	3.27	2.25	68.79	26.3	1.99	7.56	18.04	2.43	13.48	12.34	2.82	22.87
V	1.21	1.67	137.69	99.45	2.85	2.87	133.21	7.57	5.68	64.26	6.61	10.28
Cr	14.16	4.49	31.7	10.2	3.99	39.16	173.83	4.65	2.67	13.8	2.37	17.14
Co	n.d.	n.d.	n.d.	17.28	1.54	8.89	34.16	1.9	5.56	18	1.95	10.81
Cu	5.99	1.25	20.86	40.45	2.55	6.3	62.39	2.94	4.72	8.2	2.64	32.22
Ba	107.04	3.34	3.12	303.42	4.57	1.51	949.51	12.04	1.27	1153.1	30.47	2.64
	REE (ppm)											
	Jb-1a (n = 6)			SO-1 (n = 3)			SO-2 (n = 2)					
	Mean	Std dev	% Std dev	Mean	Std dev	% Std dev	Mean	Std dev	% Std dev			
La	36.39	3.21	8.83	57.98	2.79	4.81	50.08	1.05	2.1			
Ce	62.82	5.01	2.97	114.21	5.93	5.19	123.48	2.43	1.97			
Nd	26.42	2.4	9.06	52.73	3.33	6.32	63.3	0.68	1.08			
Sm	4.84	0.32	6.59	8.35	0.36	4.33	12.74	0.25	1.93			
Eu	1.55	0.12	7.4	1.78	0.1	5.39	3.82	0.07	1.79			
Dy	4.33	0.32	7.48	5.06	0.23	4.56	9.54	0.12	1.26			
Er	2.47	0.19	7.6	2.64	0.09	3.45	4.51	0.14	3			
Yb	1.98	0.16	8.32	2.14	0.11	5.24	3.40	0.08	2.18			
Lu	0.3	0.02	5.94	0.31	0.02	5.76	0.48	0.01	2.68			

canic glass in variable amounts, according to the degree of alteration. In the Zoulias profile, labradoritic plagioclase and sanidine occur as predominant phases while apatite, pyrite and/or marcasite are accessory minerals. Fresh glass is present in the least altered zones. In the Zoulias deposit, replacement of plagioclase by smectite has also been observed (Christidis et al. 1995).

Chemistry

MAJOR ELEMENTS. Alteration in the Prassa profile (Table 2) involves removal of alkalis and enrichment in Mg, Al, Ti, Fe and Ca relative to the parent rock (Figure 3a). This has been observed also during the alteration of acidic rocks both in nature (Zielinski 1982) and the laboratory (Shiraki et al. 1987). Apparently, the relative removal of alkalis, which is almost complete in the smectite zone, differentiates the smectite and the zeolite-bearing zone. Si is intensively depleted from the smectite zone and is concentrated in the smectite + opal-CT zone.

Enrichment of elements might have taken place *in situ* if they have behaved residually; that is, if they are essentially immobile, or if they have been introduced by the fluid phase. Interpretation of the behavior of elements can be made either by suitable geochemical

https://doi.org/10.1346/CCMN.1998.0460403 Published online by Cambridge University Press

Table 2. Chemical analyses of the rocks in the Prassa alteration profile. Sample SM285 corresponds to the fresh glass; SM283 to the glass + smectite zone; SM282 to the smectite + opal-CT zone; SM281, SM280, SM279 and SM278 to the smectite zone; and SM277 and SM261 to the smectite + mordenite zone. Characterization of the alteration zones is from Christidis and Scott (1997).

	SM285	SM283	SM282	SM281	SM280	SM279	SM278	SM277	SM261
					Major elements (%)				
SiO_2	72.51	71.78	76.23	63.61	61.39	61.67	60.82	64.47	67.74
Al_2O_3	12.06	13.21	11.66	19.6	20.47	21.96	20.67	19.06	16.79
TiO_2	0.09	0.1	0.11	0.18	0.16	0.18	0.17	0.15	0.13
Fe_2O_3	0.56	0.72	1.17	1.85	1.91	1.71	2.18	1.63	1.19
MnO	0.01	0.02	0	0	0	0	0.01	0	0.02
MgO	0.27	1.33	2.79	4.53	5.09	4.9	5.28	3.41	1.99
CaO	0.51	0.61	0.7	1.07	1.1	1.11	1.06	1.08	1.14
Na_2O	3.51	3	0.39	0.49	0.75	0.7	0.88	1.17	1.94
K_2O	4.19	2.82	0.12	0.12	0.21	0.13	0.33	1.69	2.3
P_2O_5	0	0.02	0.02	0.03	0.02	0	0	0	0
LOI	5.84	5.86	6.1	8.34	7.85	8.17	6.91	7.43	7.29
SO_3	0	0	0.06	0.13	0.33	0	0.81	0	0
Total	99.55	99.47	99.35	99.95	99.28	100.53	99.12	100.09	100.53
					Trace elements (ppm)				
V	4.2	5.9	0	4.7	0	6.1	6.7	4.6	2.8
Cr	20.8	4	22.4	4.8	6.2	5.9	5.1	2.5	6.3
Ni	4.4	5.7	3.2	5.3	6.7	4.9	6.1	4.5	4.9
Zn	70.2	106.5	203.3	217.4	257.3	283.8	647.8	363.4	343.2
Rb	259.3	297	5.9	9.8	12.9	4.8	20	59	116.5
Sr	172.6	163	56.1	105.6	113	104.9	179.5	130.7	97.2
Y	19.8	22.6	15.2	18	11.2	18.2	31.2	18.5	16.5
Zr	78.3	86.9	88.1	135.6	131.7	148.2	139.7	123.4	94.6
Nb	12.9	15	12.9	21.6	19.7	24	26.7	17.5	14.8
Ba	981.7	255	23.5	1422.6	1246	918.9	2994.5	1830.2	79.7
La	29.41	34.67	36.54	41.48	36.75	35.95	43.8	41.83	39.7
Ce	47.47	57.18	54.8	67.25	61.14	61.22	69.46	68.93	61.26
Nd	15.39	18.21	18.5	23.95	19.84	22.93	25.5	20.48	18.6
Sm	2.18	2.93	3.02	3.11	2.29	2.74	0	2.83	3.21
Eu	0.3	0.48	0.42	0.49	0.31	0.47	0	0.42	0.39
Dy	2.76	3.41	3.01	3.84	2.63	3.41	0	3.63	2.9
Er	2.05	2.8	1.96	2.32	1.02	2.16	0	1.92	1.84
Yb	2.3	2.81	1.74	1.99	1.26	2.05	0	1.87	1.75
Lu	0.35	0.43	0.25	0.29	0.18	0.33	0	0.28	0.25
Th	21.2	23.5	25.7	38.3	41	42.9	41.6	35.7	33.3

plots or by calculations that take into account the volume and density changes during alteration. If Al_2O_3 and TiO_2 were immobile, then they should display a linear relationship when plotted versus one another, with the straight line passing from the origin. Furthermore, the composition of the fresh rock should plot on the same trend (MacLean 1988), because the ratio of the elements remains constant. Such behavior is indeed observed (Figure 4a), indicating that the enrichment of both elements is residual. Calcium seems to have been enriched *in situ,* although the observed scatter (Figure 4b) might indicate some degree of uptake from the fluid phase.

The intercept of a regression line through the data on the ordinate will be positive if an element is lost and negative if it has been gained relative to an immobile component (Land et al. 1997). Hence, Mg and Fe have been enriched relative to Al (Figures 4c and 4d), while Si has been lost (Figure 4e). In accordance with the present study, Zielinski (1982) observed a 13–15-fold increase in the Mg-content of a rhyolite during alteration to bentonite. As expected, a positive linear trend is obtained when Mg is plotted versus Fe, which does not pass through the origin (Figure 4h). Thus, both Mg and Fe have undergone enrichment through uptake from an external source. The fresh glass plots in the lower parts of the observed trends.

The Zoulias profile is characterized by immobility of Al and Ti (Figure 5a), progressive removal of alkalis and Ca and increase of Mg- and Fe-content of the altered rock relative to Al (Table 3, Figures 3b, 5b and 5d). Si-migration is insignificant compared to the Prassa profile; P seems to migrate in the more advanced stages of alteration and loss on ignition (LOI) increases gradually with advancing alteration (Table 3). In Figure 5, the scatter of the plotted points from the line that connects the fresh rock with the origin is a measure of the degree of mobilization of chemical elements, since their concentration varies over a virtually constant Al-content of the rock.

https://doi.org/10.1346/CCMN.1998.0460403 Published online by Cambridge University Press

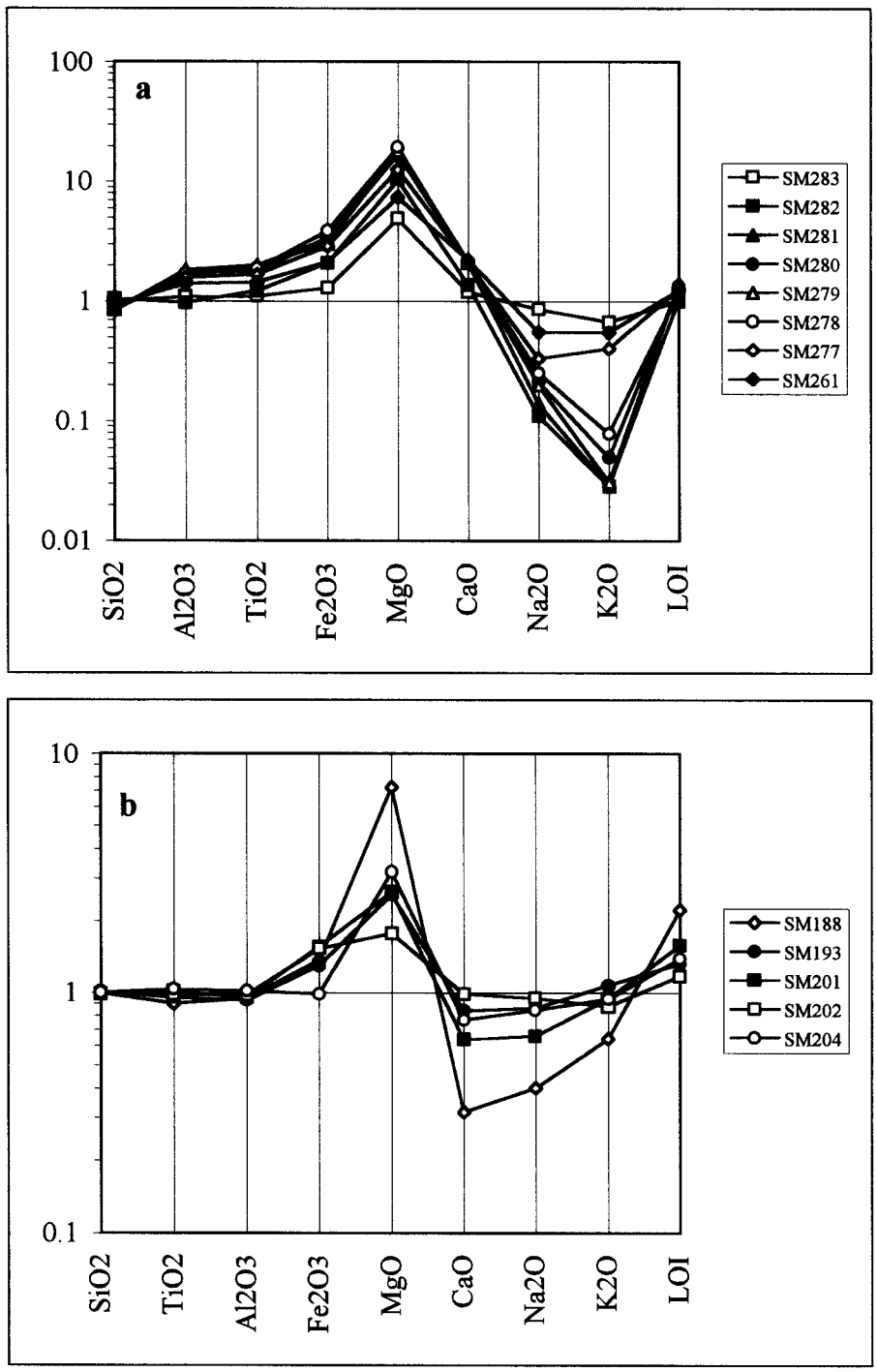

Figure 3. Multielement diagrams showing the mobility of the major chemical elements during the conversion to bentonite of a) an acidic rock (Prassa deposit, Kimolos), and b) an intermediate rock (Zoulias deposit, Milos). In both profiles, relative normalization was made over fresh glass (SM285 and SM203, respectively).

https://doi.org/10.1346/CCMN.1998.0460403 Published online by Cambridge University Press

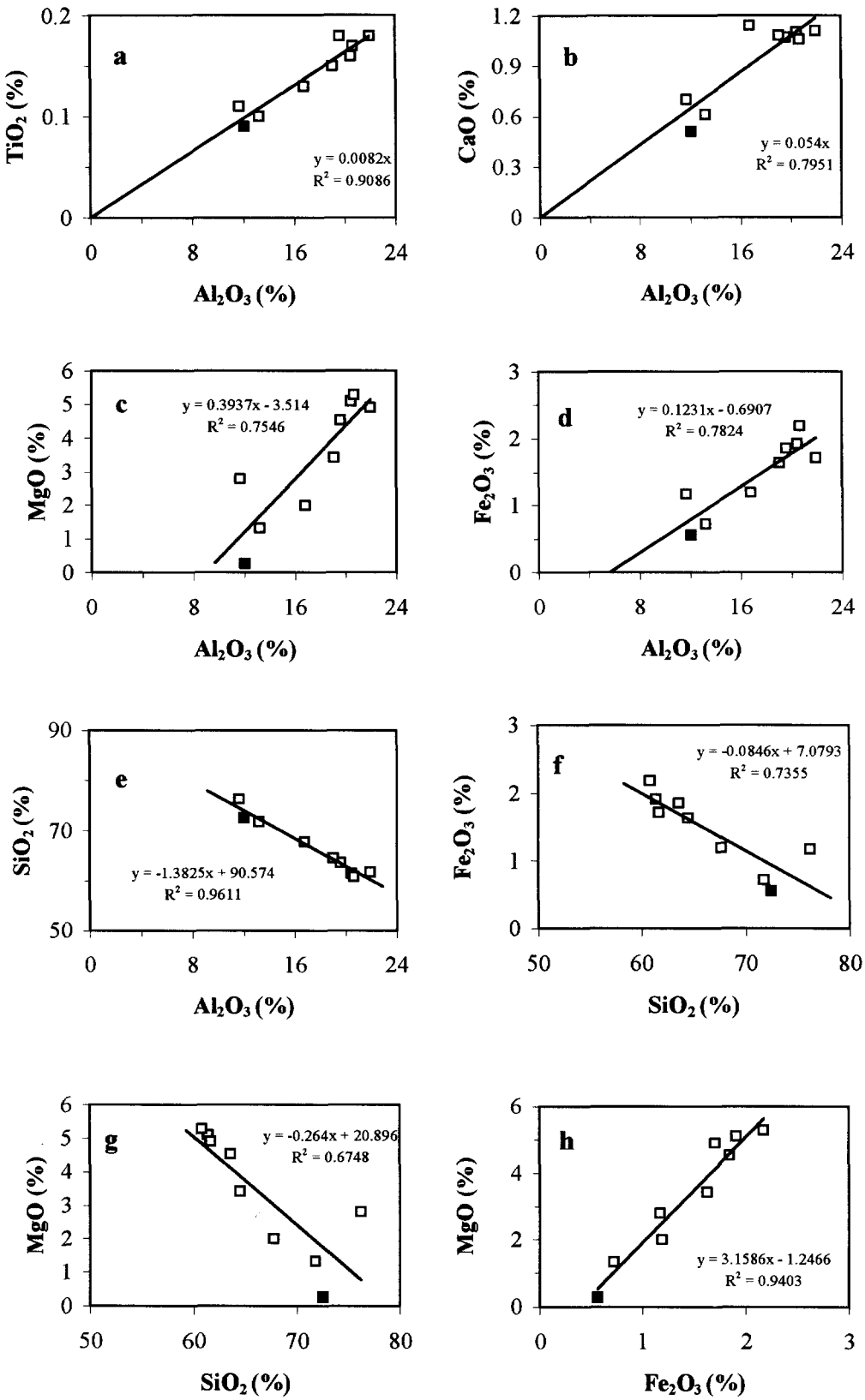

Figure 4. Projection of major elements over Al (a–e), Si (f–g) and Mg vs. Fe (h) for evaluation of their relative mobility during bentonitization in the Prassa profile. The solid square corresponds to the fresh glass.

https://doi.org/10.1346/CCMN.1998.0460403 Published online by Cambridge University Press

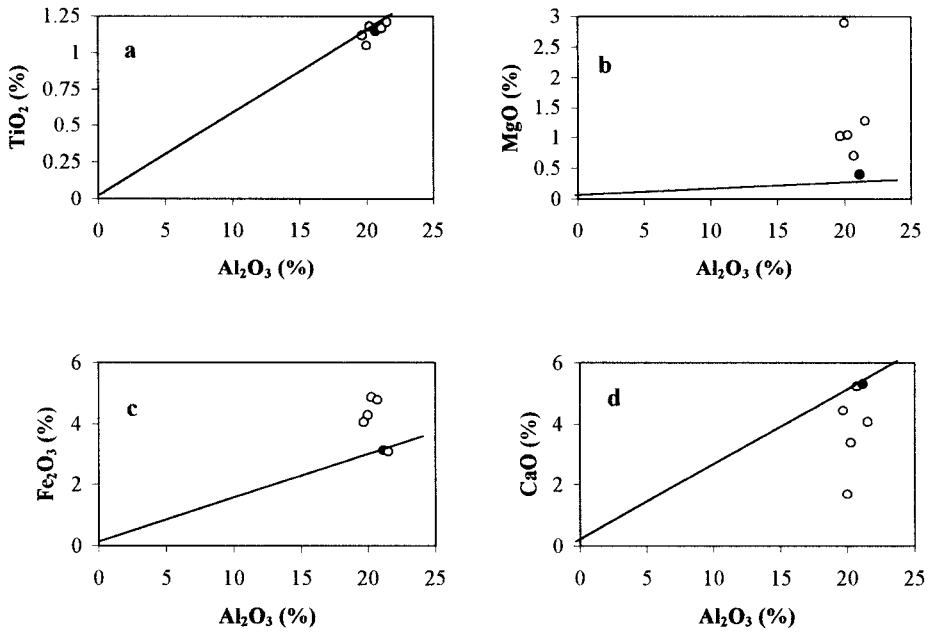

Figure 5. Projection of major elements over Al for evaluation of their relative mobility during alteration to bentonite in the Zoulias profile. The solid circle corresponds to the fresh glass.

The absolute amounts of each element gained or lost during alteration were determined using the procedure of Gresens (1967), which takes into account changes in volume and density. The weight of a chemical component X_i gained or lost by the daughter material D (bentonite) relative to the parent material P is given by the following relationship:

$$X_i = 100[f_v(g\mathrm{D}/g\mathrm{P})C_i^{\mathrm{D}} - C_i^{\mathrm{P}}] \quad [1]$$

where f_v is the volume factor ($V_{\text{daughter}} - V_{\text{parent}}$), g is the grain density and C_i is the concentration of component i. The relative percent change ($\Delta\%$) of the analyzed value of the daughter material, which normalizes the large differences in weight percent gains and losses in major and minor components, is as follows (Wintsch and Kvale 1994):

$$\Delta\% = 100[X_i/C_i^{\mathrm{P}}f_v] \quad [2]$$

The terms used in Equation [2] are those defined in Equation [1]. In both profiles, the value of f_v was calculated by considering Al immobile, that is, by taking $X_{\mathrm{Al}} = 0$ in Equation [1]. The immobility of Al has been confirmed from the results in Figures 4a and 5a. Due to the considerably lower density of the parent unwelded ignimbrite (1.62 g cm^{-3}) compared to bentonite (2.6 g cm^{-3}), the volume factors in the various zones of the Prassa profile are significantly reduced (less than 0.4 in the smectite zone). On the contrary, alteration is essentially isovolumetric in the Zoulias profile.

The values of X_i and $\Delta\%$ calculated for both profiles are given in Tables 4 and 5. Positive values indicate gain and negative values loss of chemical elements during alteration. The results confirm the information provided by the geochemical diagrams. Thus, Ti is immobile in both profiles, while Si is immobile in the Zoulias profile; the values slightly higher than ±5% (indicative of residual behavior) obtained for Ti in a few samples of the Prassa profile are explained by the increasing uncertainty induced by the low concentration of Ti in these samples. Mg and Fe have been supplied by the fluid phase, while alkalis are leached in both profiles. Ca has been supplied by the fluid phase in the Prassa profile, while it is depleted in the Zoulias profile. Also, it is interesting that, on absolute terms with advancing alteration, LOI increases as expected in the Zoulias profile and decreases in the Prassa profile.

TRACE ELEMENTS. The accuracy and precision of the analytical methods used for determination of trace elements are considerably lower compared to major elements (Table 1). Moreover, most trace elements are associated with minerals present in subordinate amounts; the distribution of these minerals affects both accuracy and precision and increases the uncertainty of measurements. Therefore, although according to Wintsch and Kvale (1994), immobile major elements should yield $\Delta\%$ values ±5%; in the case of trace elements, higher $\Delta\%$ values may also be indicative of residual behavior.

In the Prassa profile, Sr and Rb are depleted during alteration (Figure 6), while Zr and Th might be considered immobile because they display residual enrich-

https://doi.org/10.1346/CCMN.1998.0460403 Published online by Cambridge University Press

Table 3. Chemical analyses of the rocks in the Zoulias alteration profile. Sample SM203 corresponds to the fresh rock.

	SM188	SM193	SM201	SM202	SM203	SM204
			Major elements (%)			
SiO_2	59.41	60.6	59.2	58.9	59.85	59.99
TiO_2	1.05	1.12	1.18	1.15	1.17	1.21
Al_2O_3	20	19.68	20.26	20.71	21.15	21.53
Fe_2O_3	4.3	4.07	4.88	4.79	3.13	3.1
MnO	0.01	0.02	0.02	0.01	0.01	0.01
MgO	2.89	1.03	1.05	0.71	0.4	1.28
CaO	1.69	4.46	3.39	5.24	5.31	4.08
Na_2O	1.5	3.23	2.46	3.55	3.73	3.15
K_2O	1.52	2.54	2.23	2.07	2.36	2.23
P_2O_5	0.17	0.15	0.31	0.24	0.25	0.25
LOI	5.8	3.46	4.12	3.05	2.6	3.62
SO_3	1.19	—	—	—	—	—
Total	99.53	100.36	99.1	100.42	99.96	100.45
			Trace elements (ppm)			
V	244.8	305.8	301.7	280.3	334.5	302.2
Cr	48.6	67.3	67.5	66.4	70.8	72.4
Ni	30.1	20.6	26.4	13.8	19.5	15.5
Zn	81.3	20.7	66.2	119.8	187.9	125.9
Rb	34.8	99.7	63.4	41.9	67.3	52.9
Sr	174.6	291.4	195.1	295.3	326.7	230.6
Y	62.7	43.6	51.4	28.8	50.2	27.3
Zr	211.1	234.2	244.8	219.8	247.7	236.7
Nb	11.3	9.7	10.7	11.7	12.3	11.3
Ba	6859.3	664.2	550.6	554.6	651.3	507.3
La	27.12	22.13	21.67	23.81	21.98	24.09
Ce	38.9	46.18	46.62	49.11	45.63	50.2
Nd	19.6	28.65	26.77	25.94	24.2	27.17
Sm	—	6.44	5.94	5.2	5.75	5.09
Eu	1.42	2.57	1.84	1.62	1.87	1.64
Dy	11.17	7.64	8	5.59	8.15	5.69
Er	4.98	4.43	4.22	3.23	4.95	3.41
Yb	2.05	4.22	4.02	2.88	4.91	2.75
Lu	0.11	0.61	0.55	0.4	0.69	0.38
Th	6.2	10.9	11.1	13.5	13.4	10

ment (Figures 6, 7a and 7b). Contrary to these results, Zielinski (1982) observed leaching of Zr and enrichment of Sr during formation of bentonite from rhyolite. Mass balance calculations (Table 4) suggest that Nb has been mobilized from the zeolite zone (SM261, SM277) and has precipitated in the smectite zone (SM278), although in the geochemical plots Nb seems to be immobile (Figure 7c). However, the relatively high $\Delta\%$ values observed for the zeolite zone and SM278 (smectite zone) (Table 4) might be due to analytical constraints (in Table 1 a low concentration of Nb is associated with lower precision and accuracy of measurements). Thus, a 10% error in the determination of Nb in SM278 (smectite zone) and the parent rock, which is well within the precision of the method in this concentration level (Table 1), might decrease $\Delta\%$ from 56% to -2%, rendering Nb immobile. For similar reasons, the behavior of V, Cr and Ni can be interpreted to be ambiguously double negative. On the other hand, Zn displays a 3–4-fold enrichment (11-fold in the smectite zone) which cannot be explained by residual behavior (Table 4, Figure 6). Finally, Ba has been removed from the zones of incipient alteration and the zeolite zone and it seems that it has been redistributed in the smectite zone (Table 4, Figure 6).

Both the light rare earth elements (LREE) and the heavy rare earth elements (HREE) are enriched in the incipient stages of alteration (glass + smectite zone). In the more advanced stages of alteration, HREE are more depleted relative to LREE (that is, fractionation is observed), as seen in normalized plots versus both the parent rock and chondrite (Figure 8). The La:Lu ratio increases from 84:1 in the parent rock to 150:1 in the zeolite zone and as high as 204:1 in the smectite zone (SM280). Mass balance calculations (Table 4) and use of geochemical plots (Figures 9a and 9b) show that, at advanced stages of alteration, leaching of the LREE relative to Al has also taken place in the smectite zone, which however is of lesser degree. It is interesting that, in a similar study (Zielinski 1982), significant fractionation of the REE was not observed. Yttrium has an ionic radius very similar to Ho (Brook-

https://doi.org/10.1346/CCMN.1998.0460403 Published online by Cambridge University Press

Table 4. Absolute weights (X_i) and percentage ($\Delta\%$) of major and trace chemical components gained or lost relative to the parent rock (SM285) during alteration in the Prassa profile. SM283 = glass + smectite zone; SM282 = smectite + opal-CT zone; SM281–SM278 = smectite zone; SM277, SM261 = zeolite bearing zone; n.d. = not determined. Calculations were made considering that Al is immobile.

	SM283	SM282	SM281	SM280	SM279	SM278	SM277	SM261
				X_i				
SiO_2	−6.979	6.335	−33.370	−36.342	−38.642	−37.024	−31.717	−23.853
Al_2O_3	—	—	—	—	—	—	—	—
TiO_2	−0.001	0.006	0.001	0.002	0.007	0.001	0.003	0.001
Fe_2O_3	0.097	0.650	0.578	0.565	0.379	0.712	0.471	0.295
MgO	0.9449	2.616	2.517	2.729	2.421	2.811	1.888	1.159
CaO	0.047	0.214	0.148	0.138	0.100	0.109	0.174	0.309
Na_2O	−0.771	−3.107	−3.209	−3.068	−3.126	−2.997	−2.767	−2.117
K_2O	−1.616	−4.066	−4.116	−4.066	−4.119	−3.100	−3.121	−2.538
LOI	−0.490	0.469	−0.708	−1.215	−1.353	−1.808	−1.139	−0.604
V	1.186	−4.200	−1.308	−4.200	−0.850	−0.291	−1.289	−2.189
Cr	−17.148	2.368	−17.847	−17.147	−17.560	−17.824	−19.218	−16.275
Ni	0.804	−1.090	−1.139	−0.453	−1.709	−0.841	−1.553	−0.880
Zn	27.028	140.074	63.568	81.390	85.658	307.762	159.737	176.315
Rb	11.844	−253.198	−253.270	−251.700	−256.664	−247.631	−221.968	−175.620
Sr	−23.790	−114.575	−107.624	−106.025	−114.991	−67.870	−89.901	−102.783
Y	0.832	−4.079	−8.724	−13.202	−9.805	−1.596	−8.094	−7.948
Zr	1.035	12.822	5.136	−0.708	3.089	3.209	−0.220	−10.350
Nb	0.794	0.443	1.445	0.061	0.280	2.678	−1.827	−2.269
Ba	−748.899	−957.394	−106.365	−247.613	−477.057	765.453	176.337	−924.453
La	2.242	8.384	−3.888	−7.759	−9.667	−3.855	−2.943	−0.894
Ce	4.733	9.210	−6.091	−11.449	−13.849	−6.943	−3.855	−3.468
Nd	1.235	3.745	−0.653	−3.701	−2.797	−0.512	−2.432	−2.030
Sm	0.495	0.944	−0.266	−0.831	−0.675	n.d.	−0.390	0.126
Eu	0.138	0.134	0.002	−0.117	−0.042	n.d.	−0.034	−0.020
Dy	0.353	0.353	−0.397	−1.211	−0.887	n.d.	−0.463	−0.677
Er	0.506	−0.023	−0.622	−1.449	−0.864	n.d.	−0.835	−0.728
Yb	0.265	−0.500	−1.076	−1.558	−1.174	n.d.	−1.117	−1.043
Lu	0.043	−0.091	−0.172	−0.244	−0.169	n.d.	−0.173	−0.170
Th	−1.546	3.582	0.566	1.155	0.560	1.272	−0.411	0.919

ins 1989); therefore, its loss is analogous to the loss of HREE (Figures 7d and 9f, Table 4). Europium and Sm are mobile in the more advanced stages of alteration, similar to the HREE but to a lesser degree, and immobile in the first stages (Table 4, Figure 9c). Among the medium rare earth elements (MREE) and the HREE, Eu is the least leached element. Note that, in the normalized REE diagrams (Figure 8), the MREE seem to be immobile. Due to the considerably greater accuracy and precision in the determination of the REE compared to other trace elements (Table 1), the $\Delta\%$ values obtained are considered reliable.

In the Zoulias profile, V, Cr, Zr, Nb and the LREE are relatively immobile during alteration, but V and Cr tend to decrease in more advanced stages (that is, SM188 in Table 5, Figures 6d and 10). On the other hand, Zn, Rb and Sr have been leached, the latter 2 especially in the most advanced stages. Therefore, Sr follows Ca and Rb follows K during alteration (r^2 for the Sr-CaO pair is 0.85 and for the Rb-K_2O pair 0.71). Note that, in the Prassa profile, Sr does not follow Ca, probably due to its small concentration in the seawater (8 ppm compared to 412 ppm for Ca; Henderson 1990). Ni varies in a nonsystematic manner in the different stages of alteration, probably due to poor analytical precision (Table 1), because of its low concentration, or to variations in the original rock. Barium is relatively stable in the first stages of alteration (SM202, SM201, SM193) but it displays a sudden increase in concentration in the more advanced stage (SM188, Figure 6d). This behavior might not be associated with alteration of the parent rock to bentonite, but might reflect secondary processes which yielded barites deposits in the vicinity of the Zoulias bentonite. Thorium displays the opposite trend and is progressively leached with progressing alteration, contrary to the Prassa profile (Figure 6d, Table 5). Possible limited analytical precision cannot explain the $\Delta\%$ values for Th, since an estimated error of $\pm 15\%$ in the Th content for the samples SM188 and SM203 (parent material) yields a $\Delta\%$ value of −33. When plotted against Al_2O_3, Nb, Zr and V to some extent plot as a cluster of points and can be considered as parts of the line passing from the origin of the axes (Figure 10). On the other hand, in the case of both Th and Zn, the points are scattered away and plot on a line nearly normal to the Al_2O_3 axis.

https://doi.org/10.1346/CCMN.1998.0460403 Published online by Cambridge University Press

Table 4. Extended.

SM283	SM282	SM281	SM280	SM279	SM278	SM277	SM261
				Δ%			
−11.070	13.474	−119.305	−135.696	−154.787	−139.595	−110.271	−73.054
—	—	—	—	—	—	—	—
−0.882	10.492	3.324	6.665	21.634	4.020	7.976	3.324
19.987	179.043	267.716	273.299	196.625	347.561	212.193	116.888
402.21	1494.05	2416.99	2736.36	2604.37	2845.92	1762.45	953.577
10.576	64.716	75.422	73.297	56.719	58.141	85.691	134.481
−25.269	−136.496	−236.969	−236.66	−258.64	−233.398	−198.924	−133.908
−44.344	−149.651	−254.668	−262.749	−285.502	−260.826	−187.757	−134.512
−9.653	12.392	−31.443	−56.334	−67.301	−84.654	−49.157	−22.956
32.487	−154.219	−80.737	−270.744	−58.781	−18.933	−77.393	−115.731
−94.820	17.561	−222.427	−223.197	−245.205	−234.278	−232.922	−173.758
21.010	−38.212	−67.100	−27.854	−112.815	−52.250	−88.959	−44.435
44.282	307.723	234.745	313.899	354.407	1198.56	573.629	557.756
5.254	−150.59	−253.208	−262.808	−287.498	−261.086	−215.8	−150.405
−15.853	−102.374	−161.645	−166.314	−193.507	−107.502	−131.307	−132.242
4.836	−31.767	−114.228	−180.516	−143.83	−22.040	−103.057	−89.146
1.520	25.255	17.003	−2.449	11.457	11.203	−0.709	−0.020
7.080	5.291	2.904	1.289	6.312	56.760	−35.705	−39.067
−87.739	−150.401	−28.088	−68.289	−141.145	213.168	45.282	−209.121
8.767	43.961	−34.263	−71.424	−95.470	−35.833	−25.223	−6.751
11.465	29.921	−33.261	−65.299	−84.738	−39.988	−20.474	−16.223
9.227	37.524	−11.006	−65.112	−52.792	−9.094	−39.829	−29.291
26.111	66.753	−31.679	−103.185	−89.966	n.d.	−45.024	12.804
52.987	69.095	1.296	−105.917	−40.552	n.d.	−28.781	−14.708
14.716	19.739	−37.310	−118.747	−93.375	n.d.	−42.304	−54.470
28.402	−1.712	−78.718	−191.378	−122.382	n.d.	−102.70	−78.901
13.270	−33.547	−121.226	−183.36	−148.279	n.d.	−122.406	−100.704
13.987	−40.284	−127.071	−188.710	−140.056	n.d.	−124.487	−108.135
7.730	24.016	6.382	13.600	7.070	15.116	4.508	8.872

Similar to the Prassa profile, the REE elements display fractionation characterized by removal of the HREE and residual enrichment of the LREE (Figures 8d and 8f), when the precision of the analytical method is taken into account (Figures 11a and 11b, Δ% values in Table 5). The release of the HREE has taken place gradually (Figures 11c and 11d, Table 5) and in constant proportions. The behavior of Y indicates small-scale mobilization and redistribution; it has been removed during the incipient stages of alteration and concentrated in SM188, that is, the more altered material (Table 5). It is interesting that Y is perfectly correlated with Dy ($r^2 = 0.965$) and that both elements are correlated with Yb and Lu if SM188 is excluded (r^2 for the pair Y-Lu is 0.80 and for Dy-Lu is 0.88). Samarium and Eu are stable in the initial stages of alteration, but are depleted in the more advanced ones (Figure 8d, Table 5).

DISCUSSION

Alteration Patterns

MAJOR ELEMENTS. In the Prassa profile, alteration began with hydration of the rhyolitic glass (sample SM285), which did not dissolve the glass but probably involved a cation exchange between the fluid phase and the parent rock (White and Claasen 1980; White 1983; Shiraki and Iiyama 1990). Thus the relatively high LOI of SM285 might either be due to an inherent high water content of the parent rock or might be considered as the first indication for alteration, since hydration of acidic volcanic glass might not lead to formation of secondary minerals (Shiraki and Iijama 1990). Hydration was followed by leaching of alkalis and silica and uptake of Mg, Fe and Ca, whereas Al and Ti behaved residually. The uptake of $SO_4^=$ is not important quantitatively. The significant uptake of Fe from the fluid phase in both alteration profiles indicates mobilization of Fe and, therefore, reducing conditions. Such conditions are frequently observed during bentonite formation (Christidis and Dunham 1993, 1997; Christidis and Scott 1997). Thus, in the Prassa profile, alteration seems to be characterized by gain of Mg + Fe(II) + Ca and loss of Na + K + Si by the solid phase. The limited amount of $SO_4^=$ taken up was consumed in the formation of barites, gypsum and, possibly, pyrite.

The extensive removal of Si and the alkali cations from the parent rock and the corresponding uptake of Mg and Fe must have taken place through a sustained

https://doi.org/10.1346/CCMN.1998.0460403 Published online by Cambridge University Press

Table 5. Absolute weights (X_i) and percentage (Δ%) of major and trace chemical components gained or lost relative to the parent rock (SM203) during alteration in the Zoulias profile. Calculations were made considering that Al is immobile.

	SM188	SM193	SM201	SM202	SM204	SM188	SM193	SM201	SM202	SM204
			X_i					Δ%		
SiO_2	2.976	5.277	1.951	0.301	−0.919	4.702	8.203	3.122	0.493	−1.563
TiO_2	−0.060	0.034	0.062	0.004	0.019	−4.819	2.677	5.063	0.371	1.622
Al_2O_3	—	—	—	—	—	—	—	—	—	—
Fe_2O_3	1.417	1.244	1.964	1.762	−0.085	42.818	36.982	60.119	55.116	−2.755
MgO	2.656	0.707	0.696	0.325	0.857	627.937	164.450	166.708	79.580	218.203
CaO	−3.523	−0.517	−1.771	0.041	−1.302	−62.736	−9.057	−31.950	0.762	−24.961
Na_2O	−2.144	−0.259	−1.162	−0.105	−0.636	−54.348	−6.454	−29.840	−2.745	−17.346
K_2O	−0.753	0.370	−0.032	−0.246	−0.169	−30.156	14.577	−1.300	−10.208	−7.305
P_2O_5	−0.070	−0.089	0.074	−0.005	−0.004	−26.563	−33.050	28.208	−1.920	−1.797
LOI	3.534	1.118	1.701	0.515	0.956	128.514	40.027	62.670	19.388	37.434
V	−75.624	−5.858	−19.547	−48.245	−37.634	−21.379	−1.630	−5.598	−14.123	−11.453
Cr	−19.406	1.527	−0.335	−2.989	0.322	−25.919	2.007	−0.453	−4.134	0.463
Ni	12.331	2.639	8.060	−5.407	−4.274	59.796	12.591	39.593	−27.150	−22.310
Zn	−101.925	−165.654	−118.792	−65.555	−64.222	−51.295	−82.033	−60.560	−34.162	−34.793
Rb	−30.499	39.847	−1.115	−24.510	−15.334	−42.854	55.093	−1.587	−35.661	−23.193
Sr	−142.061	−13.534	−123.029	−25.126	−100.170	−41.119	−3.855	−36.074	−7.531	−31.212
Y	16.105	−3.343	3.458	−20.788	−23.382	30.338	−6.197	6.598	−40.549	−47.414
Zr	−24.462	3.994	7.854	−23.230	−15.178	−9.339	1.500	3.037	−9.183	−6.238
Nb	−0.350	−1.875	−1.130	−0.351	−1.199	−2.693	−14.188	−8.800	−2.798	−9.927
Ba	6602.410	62.512	−76.513	−84.917	−152.954	958.608	8.931	−11.253	−12.767	−23.906
La	6.699	1.803	0.642	2.336	1.685	28.822	7.633	2.798	10.406	7.803
Ce	−4.493	3.999	3.038	4.523	3.684	−9.312	8.156	6.378	9.707	8.219
Nd	−3.473	6.590	3.746	2.291	2.490	−13.571	25.339	14.828	9.270	10.476
Sm	−5.750	1.171	0.451	−0.440	−0.750	−94.563	18.950	7.512	−7.485	−13.275
Eu	−0.368	0.892	0.051	−0.216	−0.259	−18.627	44.383	2.604	−11.289	−14.096
Dy	3.662	0.061	0.201	−2.441	−2.560	42.493	0.693	2.368	−29.331	−31.981
Er	0.316	−0.189	−0.545	−1.651	−1.600	6.043	−3.555	−10.539	−32.667	−32.908
Yb	−2.742	−0.375	−0.713	−1.969	−2.209	−52.811	−7.103	−13.918	−39.264	−45.789
Lu	−0.574	−0.034	−0.116	−0.282	−0.317	−78.621	−4.644	−16.082	−39.949	−46.724
Th	−6.844	−1.686	−1.812	0.387	−3.577	−48.294	−11.706	−12.956	2.827	−27.170

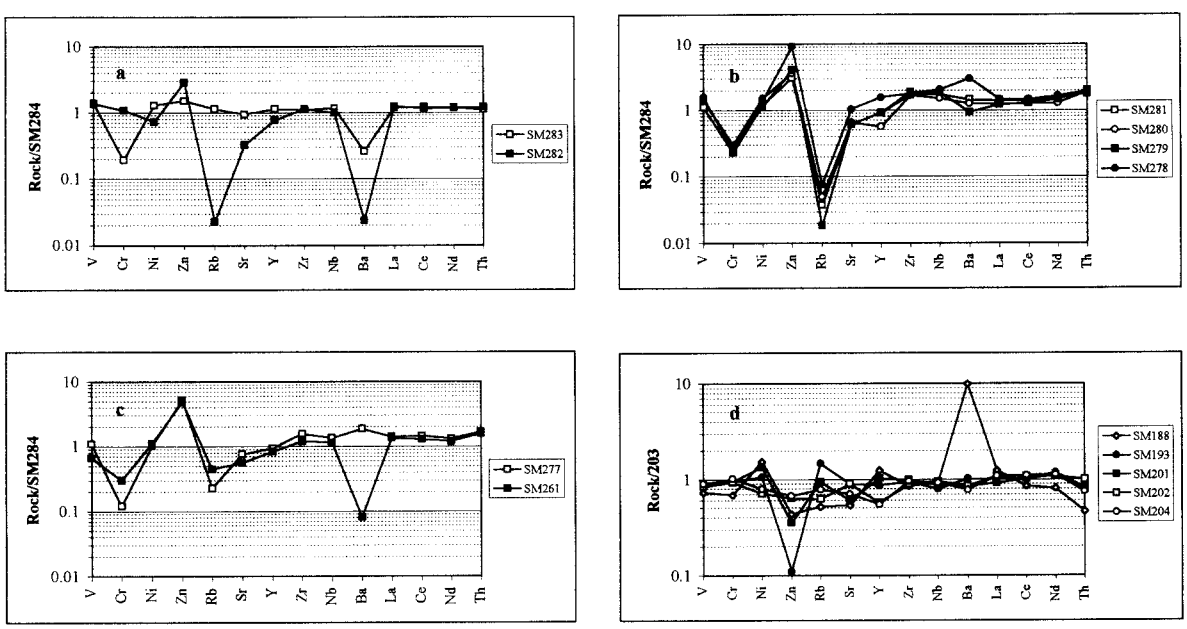

Figure 6. Multielement diagrams showing the mobility of trace elements in the alteration profiles. a) glass + smectite zone (SM283) and smectite + opal-CT zone (SM282) Prassa profile, b) smectite zone, Prassa profile, c) mordenite bearing zone, Prassa profile, d) Zoulias profile. In both profiles, normalization was made over fresh glass.

https://doi.org/10.1346/CCMN.1998.0460403 Published online by Cambridge University Press

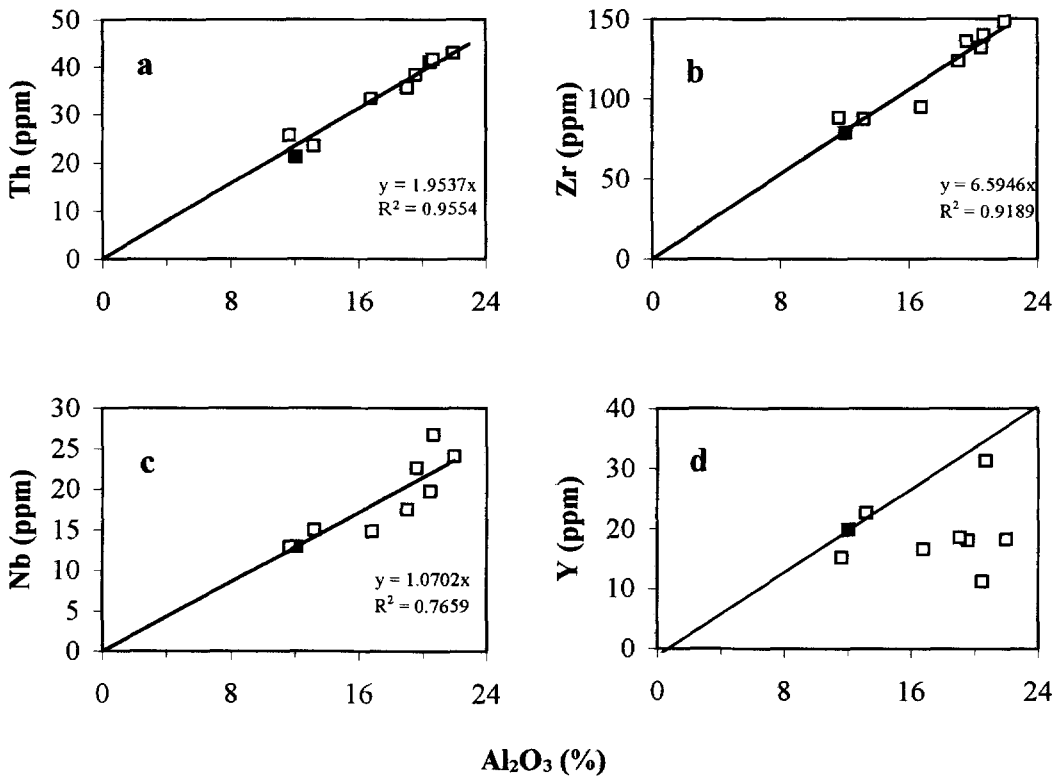

Figure 7. Projection of Th, Zr, Nb and Y over Al for evaluation of their relative mobility during bentonitization in the Prassa profile. The solid square corresponds to the fresh glass.

reaction, which also promoted significant mass transfer (Table 4). This suggests that the water : rock ratio was high, implying the existence of zones with high hydraulic conductivity in the parent material. Geological observations revealed that the alteration is structurally controlled. Such conditions are compatible with high water : rock ratios and a fully open system. The fact that maximum mass transfer is observed in the smectite zone indicates that hydraulic conductivity was probably greater in this zone.

In the Zoulias profile, alteration is characterized by leaching of alkalis and Ca and uptake of Mg, Fe and H_2O from the parent andesitic rock, while Si, Al and Ti behaved residually. Similar to the Prassa profile, significant uptake of $SO_4^=$ was not observed (Table 3). The negligible increase in the abundance of the immobile Si, Al and Ti indicates that the loss of alkalis and Ca was counterbalanced almost entirely by the uptake of Mg, Fe and H_2O.

TRACE ELEMENTS. The comparative study of the 2 alteration profiles revealed that Zr and Nb are essentially immobile, whereas Y and the HREE are both mobile. Therefore, the discrimination diagrams of Winchester and Floyd (1977) often used to determine the nature of the protoliths of rocks that have been affected by alteration, might be misleading, at least in the case of bentonite formation. In Figure 12, it is obvious that the Nb : Y ratio of the samples from the Prassa profile varies to such a degree that the samples from the smectite zone plot close to the trachyandesite-trachyte boundary, although the fresh rock has a rhyolitic/rhyodacitic composition. Thus, the removal of Y during alteration increased the Nb : Y ratio, leading to an apparent shift of the predicted parental composition to a more alkaline character. The projection of the altered rocks perpendicular to the Zr/TiO_2 axis, which expresses the basic character of the parent rock, also confirms that the different Si-content in the various zones is due to removal of Si accompanied by residual enrichment of Al. Thus, the observed basic character of the altered rocks is inherited. A similar shift of the predicted parental composition to a more alkaline character (that is, higher Nb : Y ratios), is observed for the Zoulias profile, although to a lesser extent (Figure 12). Hence, the diagram should be used cautiously for estimation of the alkaline character of the protoliths of bentonites. On the other hand, it provides a rather reliable indication of their basic character.

The fractionation of REE in both profiles indicates that there must be a sink that holds the LREE in the system, but not the HREE. In the Prassa profile this sink is a <2-μm monazite-type phosphate determined

https://doi.org/10.1346/CCMN.1998.0460403 Published online by Cambridge University Press

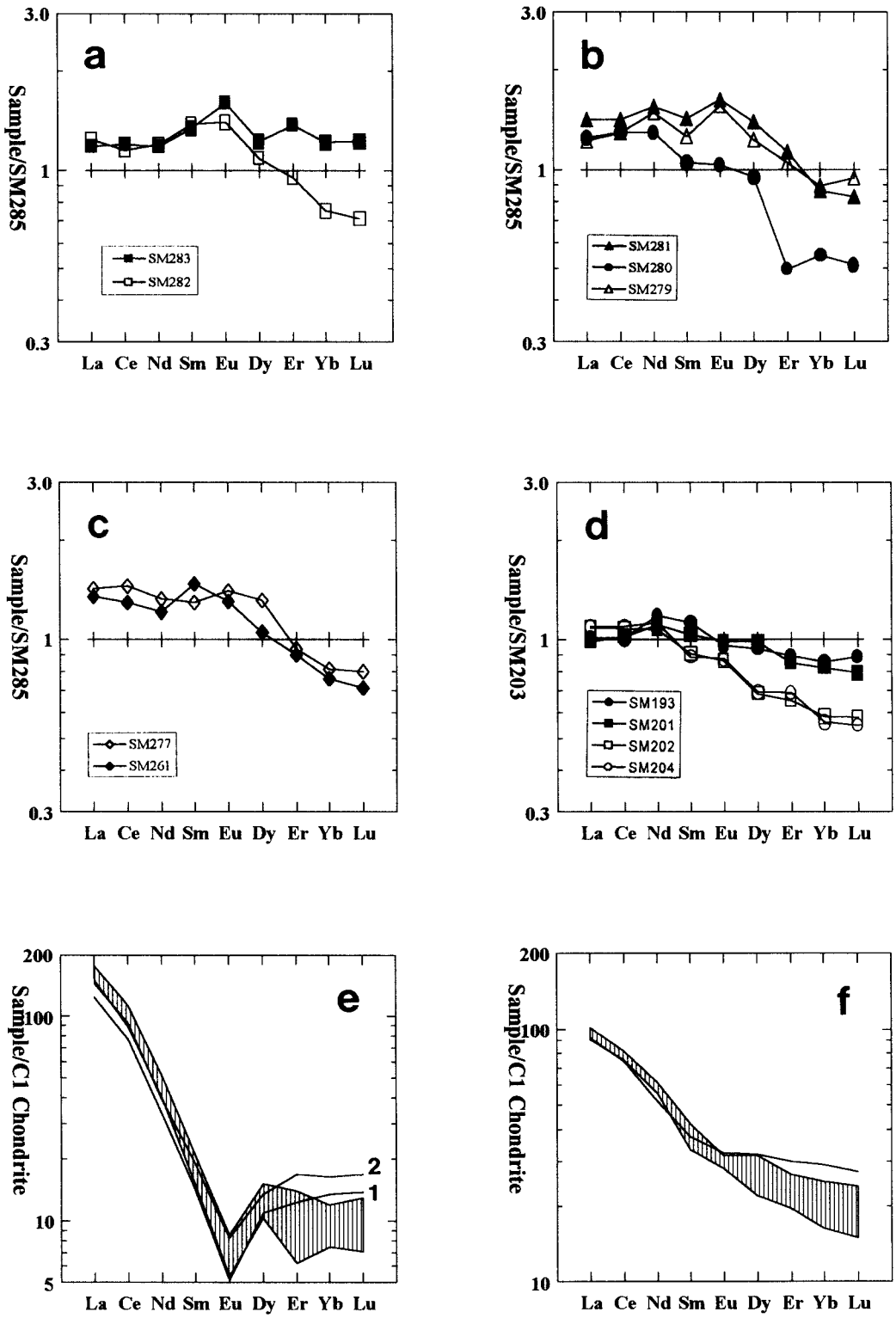

Figure 8. REE (multielement) diagrams from the 2 alteration profiles after normalization over fresh glass (a–d) and chondrite (e, f) showing the observed fractionation of the REE. a) glass + smectite zone (SM283) and smectite + opal-CT zone (SM282), Prassa profile, b) smectite zone, Prassa profile, c) mordenite-bearing zone, Prassa profile, d) Zoulias profile, e) Prassa profile, f) Zoulias profile. In e and f the hatched area corresponds to the altered samples in both profiles, the single line in the Zoulias profile and line 1 in the Prassa profile correspond to the fresh glass, while line 2 in the Prassa profile corresponds to glass + smectite zone (SM283).

https://doi.org/10.1346/CCMN.1998.0460403 Published online by Cambridge University Press

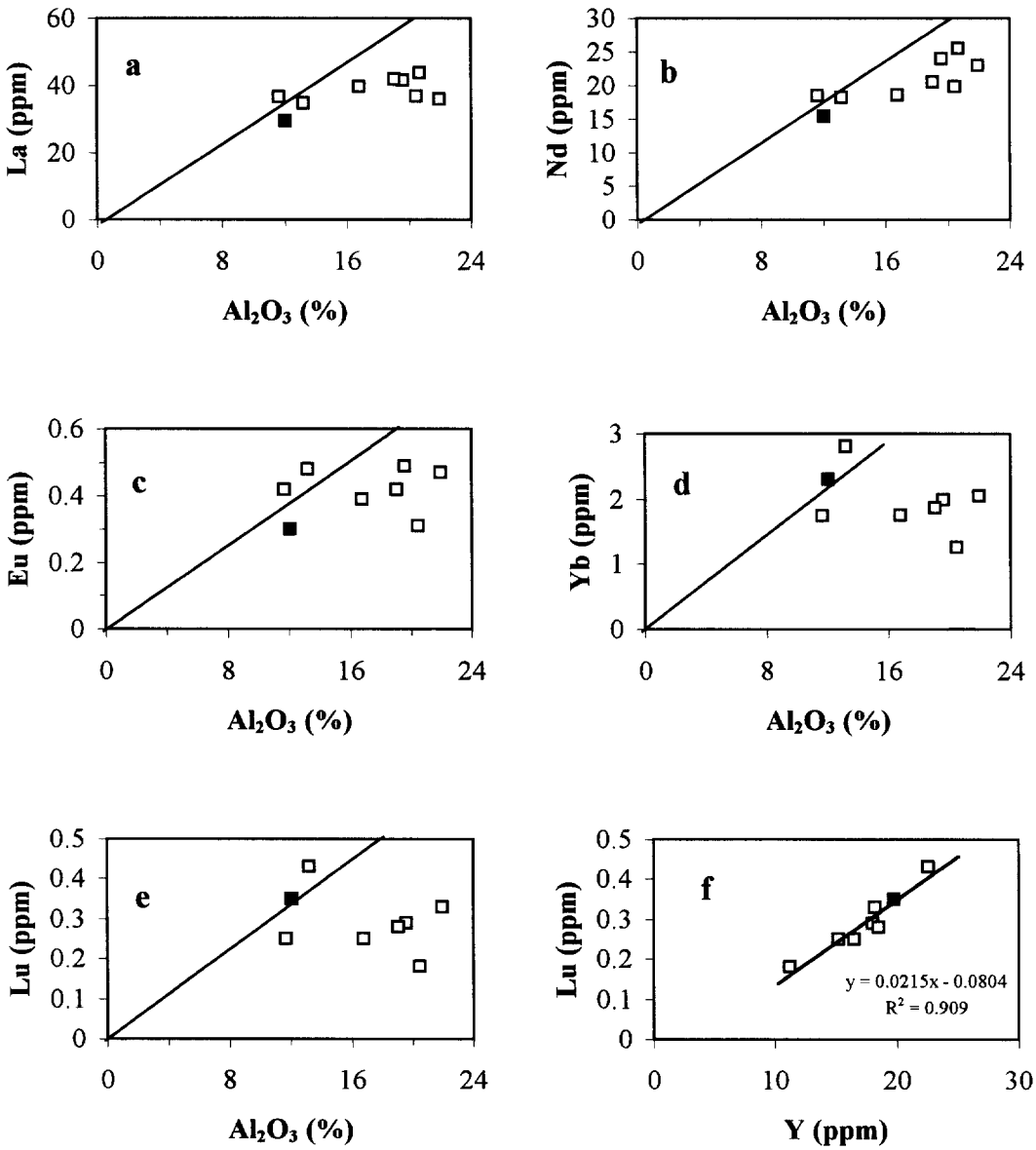

Figure 9. Projection of REE over Al (a–e), and Y vs. Lu (f). The solid square corresponds to the fresh glass (SM285).

with electron-probe micro analysis (EPMA), using backscattered electron images. Due to its fine-grained nature, it was not possible to obtain accurate analysis without interference from the smectite-rich background. The P_2O_5-content of the parent rock (SM285) is below the detection limit of the analytical method (0.02%), which corresponds to less than 0.06% monazite (Deer et al. 1962). Although such an amount of monazite can account for the LREE and Th present in the parent rock, its presence was not verified in SM285. Also, the partial removal of LREE suggests that part of these elements was initially in the glass, suggesting an, at least partly, authigenic growth of monazite. Formation of authigenic phosphates like monazite and rhabdophane has been observed during diagenesis and supergene processes (Mariano 1989; Milodowski and Hurst 1989; Milodowski and Zalasiewitz 1991).

A different reaction path took place in the Zoulias profile, in which the immobility of the LREE and P is probably due to the stability of igneous apatite present (Christidis et al. 1995). Since Th is incorporated only in small amounts in the structure of apatite, it migrates from the system. The decrease of the P-content observed in advanced stages of alteration (SM188) might reflect either alteration of apatite and adsorption of the

https://doi.org/10.1346/CCMN.1998.0460403 Published online by Cambridge University Press

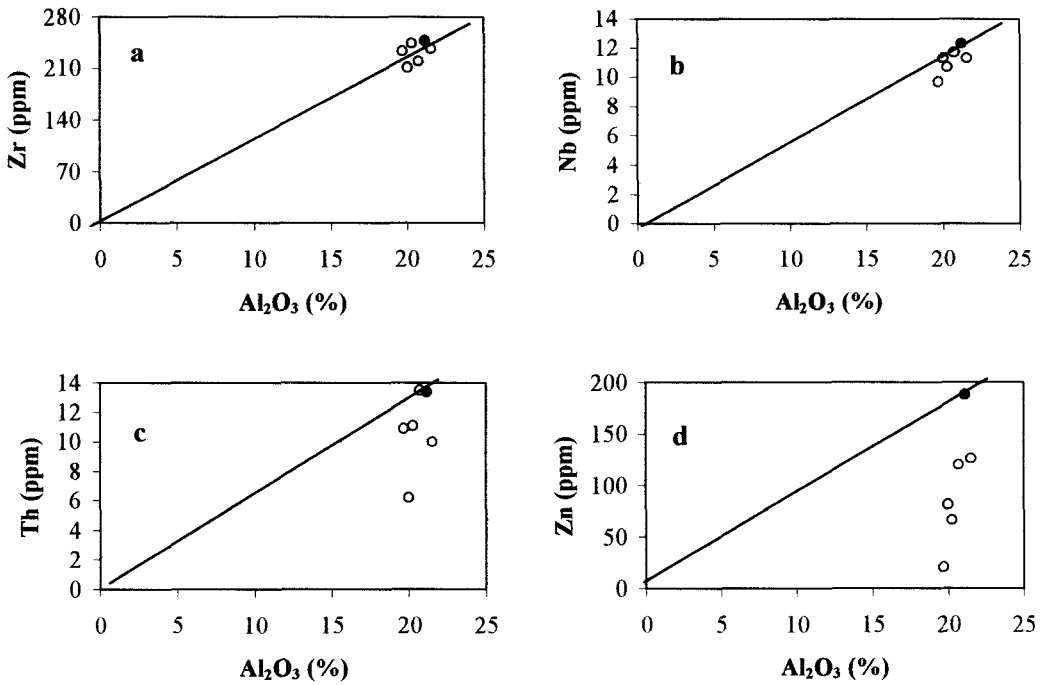

Figure 10. Projection of Zr, Nb, Zn and Th over Al for evaluation of their relative mobility during bentonitization in the Zoulias profile. The solid circle corresponds to the fresh glass (SM203).

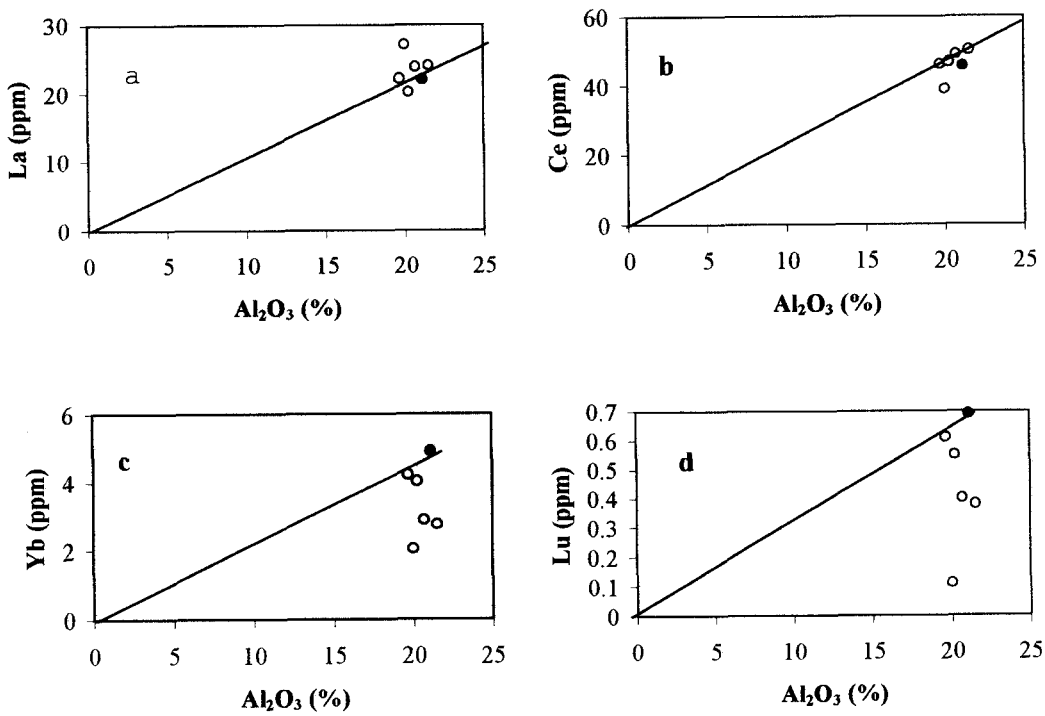

Figure 11. Projection of REE over Al in the Zoulias profile. The solid circle corresponds to the fresh glass (SM203).

https://doi.org/10.1346/CCMN.1998.0460403 Published online by Cambridge University Press

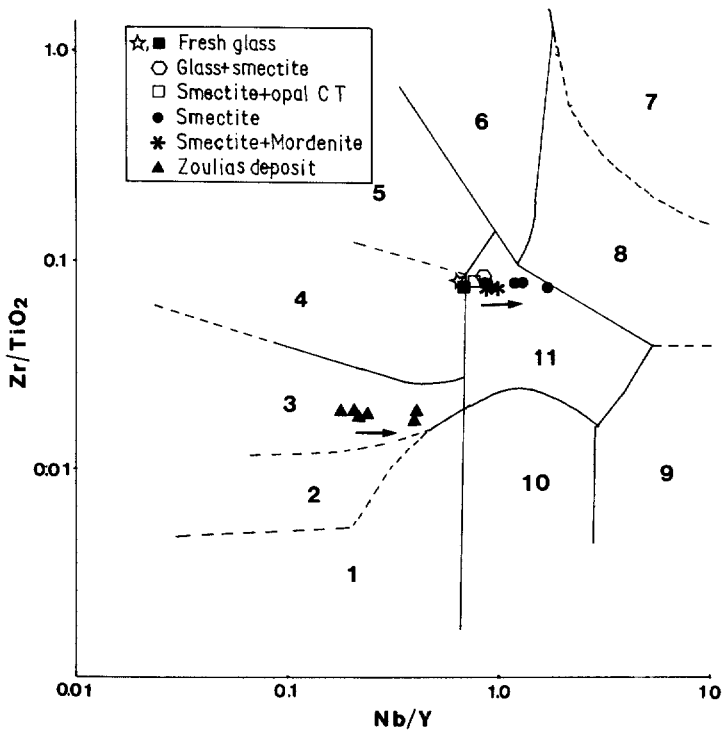

Figure 12. Projection of rocks from both profiles in the diagram of Winchester and Floyd (1977). The arrows indicate the direction of increasing degree of alteration.

LREE on other authigenic minerals like smectite and/or Fe-oxides, or merely inhomogeneity of the parent rock, because the LREE are essentially immobile throughout the whole alteration profile (Table 5).

The results obtained suggest that Th and the REE appear to enter in phosphates, although neoformed phyllosilicates might also be additional hosts as suggested in other studies (Spears and Kanaris-Sotiriou 1979; Elliott 1993). Similar observations have been made in weathering profiles and diagenetic environments (Banfield and Eggleton 1989; Milodowski and Hurst 1989; Milodowski and Zalasiewitz 1991), while Prudencio et al. (1995) reported only partial incorporation of REE in clay minerals during weathering of basalts. The HREE were initially in the glass and were subsequently leached during alteration. Therefore, the type of the authigenic minerals that form during bentonite formation might be a crucial factor causing fractionation of the REE. Minerals like monazite may modify REE patterns because they are characterized by high mineral : fluid partition coefficients and can accumulate REE (Bau 1991). Formation of such a phase might be favored under conditions of infiltration metasomatism characterized by high water : rock ratios (Bau 1991), like those that might have occured in the Prassa profile.

The significant increase of the Fe-content, especially in the smectite zone, owing to a substantial Fe-supply, indicates that Fe was transported in the ferrous state either in the form of Fe^{2+} or $Fe(OH)_3^-$ at slightly reducing conditions close to the hematite/magnetite field boundary. This is because at the neutral to slightly alkaline pH in which the bentonites formed, ferric iron is highly insoluble (Garrels and Christ 1965). Also, S is present as $SO_4^=$ and to a lesser degree as $S^=$ in pyrite. These facts impose some constraints on the valence state of the REE, especially of Ce and Eu. The Eh/pH conditions and the low temperature of alteration suggest that Ce and Eu should be present in their trivalent state (Sverjensky 1984; Brookins 1989), although the significance of Eu^{2+} in higher temperatures is increased (Wood 1990b). The presence of Eu^{3+} even at slightly reducing conditions at low temperatures is due to complexation (Wood 1990b; Bau 1991). Moreover, in the Zoulias profile, the removal of Eu in more advanced stages of alteration is probably due to the replacement of labradorite by smectite (Christidis et al. 1995).

The removal of the REE from both profiles was probably assisted by complexation of the leached elements. The complexes that might be present at the existing Eh/pH conditions would be carbonates (Cantrell and Byrne 1987; Wood 1990a, 1990b). Chloride (Brookins 1989; Wood 1990b) sulphate (Brookins 1989; Wood 1990a) and especially fluoride (Wood 1990b) complexes might become important at low pH

https://doi.org/10.1346/CCMN.1998.0460403 Published online by Cambridge University Press

Table 6. Calculated water : rock (WR) ratios in the Prassa and Zoulias alteration profiles. Zoulias calculations were based only on the amount of Mg taken up, because Ca was released during alteration. See text for discussion.

Alteration zones	WR ratio based on Mg-uptake	WR ratio based on Ca-uptake
Prassa profile (rhyolitic precursor)		
Smectite zone	13.3 : 1	2 : 1
Zeolite bearing zone	5.5 : 1	5.5 : 1
Glass + smectite zone	4.5 : 1	0.9 : 1
Zoulias profile (andesitic precursor)		
Smectite-rich bentonite	12.6 : 1	—
Slightly altered material	1.6 : 1	—

in some hydrothermal systems (Brookins 1989; Wood 1990b), but are not important at the physicochemical conditions under which alteration took place.

Mineralogical Control of the Alteration

The gains/losses of major elements during alteration in both profiles depend on the nature of the parent rock and the composition of the fluid phase and control the type of the authigenic minerals formed. The elements released during alteration reflect the influence of the composition of the parent rock. Although andesites are richer in Ca and poorer in Si than rhyolites, Chambers-type montmorillonite is the major authigenic mineral in both profiles (Christidis and Dunham 1993; Christidis and Scott 1997). In the Prassa profile, the Si : Al ratio of the parent glass (Table 2) is considerably higher compared to Chambers-type montmorillonite. Therefore, in order to form smectite-rich, opal-CT-poor bentonites, the excess silica has either to be leached or incorporated into a mordenite structure having a Si : Al ratio between 4.8 and 5.8 (that is, identical to the value of 5.1 of the original ignimbrite). Thus, depletion of Si is less intense in the zeolite zone. The massive depletion of Si indicates removal via advection rather than diffusion, which is compatible with a control of the alteration by faults (structurally controlled alteration).

In the Zoulias profile, the Si : Al ratio of the parent rock is almost identical to that of Chambers-type montmorillonite. Therefore, silica has been incorporated in smectite and neither Si-migration nor formation of Si-rich phases was observed. Similarly, Ca is progressively leached in the Zoulias profile during alteration of glass and plagioclase, because its abundance in the parent rock is considerably higher compared to the neoformed smectite. An opposite trend is observed in the Prassa profile because the parent rock was a rhyolite. Significant Ca-uptake during alteration of rhyolite is well known from experiments (Shiraki et al. 1987). Alkalis are depleted in both profiles and, in the Prassa profile, release of alkalis in the zeolite zone takes place to a lesser degree compared to the smectite zone. Such a behavior is expected since zeolites instead of smectite are favored by high (Na + K)/H activity ratios (Hess 1966).

The type of elements taken up during alteration depends on the composition of the fluid phase. In both profiles, the Mg and Fe taken up are incorporated principally in the neoformed montmorillonite (Christidis and Dunham 1993; Christidis and Scott 1997), since only small amounts of Fe have been incorporated in pyrite and Fe-oxides. Crystallization of smectite is expected to be fast and contemporary with alteration of volcanic glass at high supersaturation conditions. The latter conditions explain the pseudomorphic replacement textures over the precursor glass (Dibble and Tiller 1981), like those observed in the Miloan bentonites (Christidis et al. 1995).

The Prassa profile represents a characteristic case of bentonite formation in which the chemistry of the parent rock does not control the type of smectite formed, because the Mg-and Fe-content of the parent rock are considerably lower compared to Chambers-type montmorillonite. Moreover, the chemical variation of the smectites formed is insignificant. On Milos Island, acidic parent rocks similar to the Prassa ignimbrite yielded smectites with composition ranging between beidellite and Tatatilla-type montmorillonite (Christidis and Dunham 1997). The significant enrichment of the altered rock in Mg (Table 4), indicates a pore fluid rich in Mg and suggests that the introduction of Mg and Fe homogenized the pore fluid chemistry and restricted the compositional variation of smectites. Since alteration took place in a marine environment, the fluid phase was probably modified seawater.

Water : Rock Ratios During Alteration

The $\Delta\%$ values obtained from Equations [1] and [2] were utilized to calculate the water : rock (WR) ratios that prevailed during bentonite formation in both profiles, using Mg as index element. The Mg-content of seawater was taken from Henderson (1990). In the calculations, it was considered that virtually all Mg present in the seawater was taken up by the neoformed smectite (Shiraki et al. 1987). The results are shown in Table 6. The calculated WR ratios in the smectite zone at the Prassa profile (13.3:1) and the Zoulias profile (12.6:1) are almost identical, suggesting that 1) the formation of smectite-rich bentonites requires high WR ratios regardless of the composition of the parent rock, 2) the formation of smectite-rich bentonites might not depend only on the composition of the parent rock as is usually assumed (Grim and Güven 1978; Christidis and Dunham 1997) and 3) high WR ratios tend to homogenize differences in the composition of the parent rocks (compare SM280 in Table 2 and SM188 in Table 3) and explain the observed mass transfer. However, the WR ratios obtained might represent maximum values. Christidis et al. (1995) con-

https://doi.org/10.1346/CCMN.1998.0460403 Published online by Cambridge University Press

sidered that the Miloan bentonites formed from a vigorous reaction between hot pyroclastic rocks and cold seawater. Such a reaction is expected to cause evaporation of seawater, raising the Mg-content of the reacting fluid.

The WR ratio in the zeolite-bearing zone is considerably lower than the smectite zone (5.5:1) and is even lower in the smectite + glass zone (4.5:1). These lower WR ratios are correlated with the smaller degree of leaching of alkalis and uptake of Mg and Fe, indicating that, in the Prassa profile, the different alteration zones are a function of the WR ratio, which in turn controls the degree of leaching of elements. Note that, in the Zoulias profile, the calculated WR ratio of the least altered samples is considerably lower (1.6:1). Also, when Ca is used for calculation of the WR ratios in the Prassa profile, different values are obtained. Thus, in the smectite zone, the WR ratio is 2:1; in the zeolite-bearing zone, 5.5:1; and in the smectite + glass zone, 0.9:1. The considerably lower WR ratios obtained for the smectite zone reflect the lower amounts of Ca taken up during bentonite formation, compared with Mg (Table 4), in accordance with the experimental work of Shiraki et al. (1987). The matching of the WR ratios in the zeolite-bearing zone reflects the lower Mg-uptake and Si-removal, through the formation of smaller amounts of smectite, which in turn is associated with the formation of mordenite.

CONCLUSIONS

The geochemical study of the progressive alteration of a rhyolite and an andesite to bentonite led to the following conclusions:

1) The conversion of volcanic rocks to bentonite is associated with migration of major and trace chemical elements from the parent rocks. Alkalis are leached, Mg and Fe are taken up and Al and Ti are immobile and are enriched residually irrespective of the nature of the parent rock. On the contrary, the behavior of Ca and Si depends on the chemistry of the parent rock. Formation of high-quality bentonites from acidic rocks (Prassa profile) results in massive removal of Si and uptake of Ca. On the other hand, Si is immobile from intermediate rocks (Zoulias profile), while Ca is leached.

2) Zr, Nb, V and Ni are residually enriched. Thorium is immobile in the Prassa profile but is leached in the Zoulias profile, while Y is mobilized in both profiles. This observation, coupled with the immobility of Nb, renders the utility of discrimination diagrams proposed by Winchester and Floyd (1977) questionable, at least as far as the alkaline character of the parent rocks is concerned.

3) The REE display fractionation in both profiles. The LREE are relatively immobile or less mobile than the HREE, which are essentially leached, especially in the more advanced stages of alteration. The observed difference is attributed to the existence of characteristic minerals like monazite (Prassa profile) and apatite (Zoulias profile), which act as sink for the LREE. The existence of monazite, which might be partly authigenic, explains the observed immobility of Th. Lack of monazite is associated with leaching of Th relative to the LREE. In any case, smectite does not seem to be the main host for REE and Th.

4) The formation of smectite-rich bentonites is associated with high WR ratios (about 13:1), regardless of the composition of the parent rock. On the contrary, formation of zeolite-bearing bentonites takes place at considerably lower WR ratios (5.5:1) and reflects a smaller Mg-uptake and alkali- and Si-removal during alteration. Therefore, the formation of smectite or mordenite appears to be affected by the WR ratio, which in turn might control the degree of leaching of the various elements.

5) High WR ratios tend to homogenize differences in composition of the parent rock, yielding smectites and, subsequently, bentonites with similar chemical characteristics. Thus, the association of particular smectites with specific rock types is not always plausible.

ACKNOWLEDGMENTS

Research was financially supported by the Greek State Scholarship Foundation (S.S.F). S. Wood revised an earlier version of the manuscript and improved the English. The author is grateful to the Silver and Barites Ore Mining Co. and Roussos Bros S.A. Greece for permitting sample collection from their quarries. The constructive reviews of W.D. Huff, R.A. Zielinski and W.C. Elliott improved the text.

REFERENCES

Altaner SP, Grim RE. 1990. Mineralogy, chemistry and diagenesis of tuffs in the Sucker Creek Formation (Miocene), Eastern Oregon. Clays Clay Miner 38:561–572.

Banfield JF, Eggleton RA. 1989. Apatite replacement and rare earth mobilization, fractionation and fixation during weathering. Clays Clay Miner 38:77–89.

Bau M. 1991. Rare-earth element mobility during hydrothermal and metamorphic fluid-rock interaction and the significance of the oxidation state of europium. Chem Geol 93: 219–230.

Bennett H, Oliver GJ. 1976. Development of fluxes for the analysis of ceramic materials by X-ray Spectrometry. Analyst 101:803–807.

Boles JR, Surdam RC. 1979. Diagenesis of volcanogenic sediments in a Tertiary saline lake, Wagon Red Formation. Am J Sci 279:832–853.

Brookins DG. 1989. Aqueous geochemistry of rare-earth elements. In: Lipin BR, McKay GA, editors. Rev Mineral 21, Geochemistry and mineralogy of rare earth elements. Mineral Soc Am. p 201–225

Cantrell KJ, Byrne RH. 1987. Rare earth element complexation by carbonate and oxalate ions. Geochim Cosmochim Acta 51:597–606.

Cas RAF, Wright JV. 1988. Volcanic successions. Modern and ancient. London: Unwin Hyman. 528 p.

Christidis G, Dunham AC. 1993. Compositional variations in smectites: Part I. Alteration of intermediate volcanic rocks.

https://doi.org/10.1346/CCMN.1998.0460403 Published online by Cambridge University Press

A case study from Milos Island, Greece. Clay Miner 28: 255–273.
Christidis G, Dunham AC. 1997. Compositional variations in smectites: Part II. Alteration of acidic precursors. A case study from Milos Island, Greece. Clay Miner 32:253–270.
Christidis G, Scott PW, Marcopoulos T. 1995. Origin of the bentonite deposits of Eastern Milos, Aegean, Greece. Geological, mineralogical and geochemical evidence. Clays Clay Miner 43:63–77.
Christidis G, Scott PW. 1997. The origin and control of colour of white bentonites from the Aegean Islands of Milos and Kimolos, Greece. Mineral Deposita 32:271–279.
Deer WA, Howie RA, Zussmann J. 1962. Rock forming minerals, vol. 5, Non silicates. Longman. p 339–346.
Dibble WE Jr, Tiller W. 1981. Kinetic model of zeolite paragenesis in tuffaceous sediments. Clays Clay Miner 29:323–330.
Duddy IR. 1980. Redistribution and fractionation of rare earth and other elements in a weathering profile. Chem Geol 30: 363–381.
Elliott WC. 1993. Origin of the Mg-smectite at the Cretaceous/Teriary (K/T) boundary at Stevns Klint, Denmark. Clays Clay Miner 41:442–452.
Fyticas M. 1977. Geological and geothermal study of Milos Island [Ph.D. thesis]. Thessaloniki, Greece: Univ of Thessaloniki. 228 p (in Greek).
Fyticas M, Innocenti F, Kolios N, Manetti P, Mazzuoli R, Poli G, Rita F, Villari L. 1986. Volcanology and petrology of volcanic products from the island of Milos and neighbouring islets. J Volcanol Geotherm Res 28:297–317.
Fyticas M, Vougioukalakis G. 1993. Volcanic structure and evolution of Kimolos and Polyegos (Milos Island group). Bull Geol Soc Greece 28:221–237.
Garrels RM, Christ CL. 1965. Solutions minerals and equilibria. San Francisco: Freeman Cooper. p 172–267.
Gresens RL. 1967. Composition-volume relationships of metasomatism. Chem Geol 2:47–65.
Grim RE, Güven N. 1978. Bentonites. New York: Elsevier. 256 p.
Hay RL. 1977. Geology of zeolites in sedimentary rocks. In: Mumpton FA, editor. Rev Mineral 4, Natural zeolites. Mineral Soc Am. p 53–64.
Hay RL, Guldman SG. 1987. Diagenetic alteration of silicic ash in Searles lake, California. Clays Clay Miner 35:449–457.
Henderson P. 1990. Inorganic geochemistry. Oxford: Pergamon Pr. p 278–303.
Henderson JH, Jackson ML, Syers JK, Clayton RN, Rex RW. 1971. Cristobalite authigenic origin in relation to montmorillonite and quartz origin in bentonites. Clays Clay Miner 19:229–238.
Hess PC. 1966. Phase equilibria of some minerals in the K_2O-Na_2O-Al_2O_3-SiO_2-H_2O system at 25 °C and 1 atmosphere. Am J Sci 264:289–309.
Iijima A. 1980. Geology of natural zeolites and zeolitic rocks. Proc 5th Int Conf on Zeolites. p 103–118.
Land LS, Mack LE, Milliken KL, Lynch FL. 1997. Burial diagenesis of argillaceous sediment, south Texas Gulf of Mexico sedimentary basin: A reexamination. Bull Geol Soc Am 109:2–15.
MacLean WH. 1988. Rare earth element mobility at constant inter-REE ratios in the alteration zone at the Phelps Dodge massive sulphide deposit, Matagami, Quebec. Mineral Deposita 23:231–238.
Mariano AN. 1989. Economic geology of rare earth minerals. In: Lipin BR, McKay GA, editors. Rev Mineral 21, Geochemistry and mineralogy of rare earth elements. Mineral Soc Am. p 309–337.
Mariner RH, Surdam RA. 1970. Alkalinity and formation of zeolites in saline alkaline lakes. Science 170:977–980.
Milodowski AE, Hurst A. 1989. The authigenesis of phosphate minerals in some Norwegian hydrocarbon reservoirs: Evidence for the mobility and redistribution of rare earth elements (REE) and Th during sandstone diagenesis. In: Miles DL, editor. Water-rock interaction WRI-6. Rotterdam: Balkema. p 491–494.
Milodowski AE, Zalasiewicz JA. 1991. Redistribution of rare earth elements during diagenesis of turbidite/hemipelagite mudrock sequences of Llandovery age from central Wales. In: Morton AC, Todd SP, Haughton PDW, editors. Developments in sedimentary provenance studies. Geol Soc Spec Publ 57:101–124.
Mottl MJ, Holland HD. 1978. Chemical exchange during hydrothermal alteration of basalt by seawater. I. Experimental results for major and minor components of seawater. Geochim Cosmochim Acta 42:1103–1115.
Mumpton FA. 1977. Utilization of natural zeolites. In: Mumpton FA, editor. Rev Mineral 4, Natural zeolites. Mineral Soc Am. p 177–204.
Noh HJ, Boles JR. 1989. Diagenetic alteration of perlite in the Guryongpo area, Republic of Korea. Clays Clay Miner 37:47–58.
Pickering KT, Marsh NG, Dickie B. 1993. Data report: Inorganic major, trace, and rare earth element analyses of the muds and mudstones from site 808. In: Hill IA, Taira A, Firth JV, et al. Proc Ocean Drilling Program, Scientific Results 131:427–432.
Prudencio MI, Gouveia MA, Sequeira Braga MA. 1995. REE distribution in present day and ancient surface environments of basaltic rocks (Central Portugal). Clay Miner 30: 239–248.
Senkayi AL, Dixon JB, Hossner LR, Abder-Ruhman, M, Fanning DS. 1984. Mineralogy and genetic relationships of tonstein, bentonite and lignitic strata in the Eocene Yegna Formation of East-Central Texas. Clays Clay Miner 32: 259–271.
Seyfried WE Jr, Mottl MJ. 1982. Hydrothermal alteration of basalt by seawater under seawater-dominated conditions. Geochim Cosmochim Acta 46:985–1002.
Sheppard RA, Gude III AJ. 1968. Distribution and genesis of authigenic silicate minerals in tuffs of Pleistocene lake Tecopa, Inyo County, California. US Geol Survey Prof Paper 597. 38 p.
Sheppard RA, Gude III AJ. 1973. Zeolites and associated authigenic silicate minerals in tuffaceous rocks of the Big Sandy Formation, Mohave County, Arizona. US Geol Survey Prof Paper 830. 36 p.
Shiraki R, Sakai H, Endoh M, Kishia N. 1987. Experimental studies on rhyolite- and andesite-seawater interactions at 300 °C and 1000 bars. Geochemical J 21:139–148.
Shiraki R, Iiyama T. 1990. Na-K ion exchange reaction between rhyolitic glass and (Na,K)Cl aqueous solution under hydrothermal conditions. Geochim Cosmochim Acta 54: 2923–2931.
Spears DA, Kanaris-Sotiriou R. 1979. A geochemical and mineralogical investigation of some British and other European tonsteins. Sedimentology 26:407–425.
Steefel CI, van Cappellen P. 1990. A new kinetic approach to modeling water-rock interaction: The role of nucleation, precursors and Ostwald ripening. Geochim Cosmochim Acta 54:2657–2677.
Surdam RC. 1977. Zeolites in closed hydrological systems. In: Mumpton FA, editor. Rev Mineral 4, Natural zeolites. Mineral Soc Am. p 65–91.
Sverjensky DA. 1984. Europium redox equilibria in aqueous solution. Earth Planet Sci Lett 67:70–78.

https://doi.org/10.1346/CCMN.1998.0460403 Published online by Cambridge University Press

Taylor MW, Surdam RC. 1981. Zeolite reactions in the tuffaceous sediments at Teels Marsh, Nevada. Clays Clay Miner 29:341–352.

Walsh JN, Buckley F, Barker J. 1981. The simultaneous determination of the REE's in rocks using ICP source spectrometry. Chem Geol 33:141–153.

White AF, Claasen HC. 1980. Kinetic model for the short-term dissolution of a rhyolitic glass. Chem Geol 28:91–109.

White AF. 1983. Surface chemistry and dissolution kinetics of glassy rocks at 25 °C. Geochim Cosmochim Acta 47: 805–815.

Wintsch RP, Kvale CM. 1994. Differential mobility of elements in burial diagenesis of siliciclastic rocks. J Sed Res A64:349–361.

Winchester JA, Floyd PA. 1977. Geochemical discrimination of different magma series and their differentiation products using immobile elements. Chem Geol 20:325–343.

Wood SA. 1990a. The aqueous geochemistry of the rare-earth elements and yttrium. 1. Review of available low-temperature data for inorganic complexes and the inorganic REE speciation of natural waters. Chem Geol 82:159–186.

Wood SA. 1990b. The aqueous geochemistry of the rare-earth elements and yttrium. 2. Theoretical predictions of speciation in hydrothermal solutions at 350 °C at saturation water vapour pressure. Chem Geol 88:99–125.

Zielinski RA. 1982. The mobility of uranium and other elements during alteration of rhyolite ash to montmorillonite: A case study in the troublesome formation, Colorado, USA. Chem Geol 35:185–204.

(Received 16 August 1996; accepted 29 September 1997; Ms. 2801)

https://doi.org/10.1346/CCMN.1998.0460403 Published online by Cambridge University Press